[American Journal of Science, Vol. 318, April, 2018, P. 409–434, DOI 10.2475/04.2018.02]

EARTH'S OLDEST PRESERVED K-BENTONITES IN THE *CA.* 2.1 Ga FRANCEVILLIAN BASIN, GABON

OLABODE M. BANKOLE*,†, ABDERRAZAK EL ALBANI*, ALAIN MEUNIER*, FLORENT PAMBO**, JEAN-LOUIS PAQUETTE§, and ANDREY BEKKER§§

ABSTRACT. Bentonites are the alteration product of volcanic tephra typically preserved in low-energy, sedimentary environments below baseline. Although volcanic tuffs occur throughout the Earth's history, bentonites older than *ca.* 1.5 Ga have not been described. We present the mineralogy, geochemistry, and age data for K-bentonite beds within the FB Formation in the unmetamorphosed Paleoproterozoic Francevillian Basin, Gabon. The clay mineralogy of the K-bentonites consists predominantly of illite with substantial amounts of kaolinite and trace amounts of long-ordered illite/smectite (R3) mixed layer. The kaolinite content and co-existing 1M and $2M_1$ illites are indicative of diagenetic smectite illitization over a prolonged period of time with minimal burial temperature. Their chemical characteristics suggest derivation from calc-alkaline intermediate to felsic magma, related to continental volcanic arc magmatism in a subduction setting. The zircon grains are relatively small, rounded to sub-rounded, and yield $^{207}Pb/^{206}Pb$ dates that have a narrow range with a weighted mean of 2971 ± 13 Ma, consistent with the age of the underlying crystalline calc-alkaline Archean basement granitoids. This age indicates incorporation of zircons from the Archean basement granitoids into the magma during magmatic activity. Considering that the FB Formation bentonites were derived from a volcanic arc developed along the margin of the West Gabonian block and are preserved in the lower part of the Francevillian Basin, we infer that this basin reflects high-rate, but short-lived sedimentation in a pro-foreland basin setting. Paleogeographically, these K-bentonites could thus serve as a potential correlation marker for the Paleoproterozoic Gabonian and adjacent cratons at *ca.* 2.1 Ga. Based on the current records, these are the world's oldest bentonite beds so far reported.

Keywords: Bentonites, clay mineralogy, U-Pb zircon geochronology, Bulk rock geochemistry, Paleoproterozoic, Francevillian Basin, Gabon

INTRODUCTION

Bentonites are smectite-dominated clay rocks that are formed by alteration of volcanic ash (tephra/tuff) under the influence of basin fluids and/or *in situ* hydrothermal alteration of pyroclastic rocks (Grim and Güven, 1978; Huff, 2016). Tephra is the explosive volcanic product that is deposited over a relatively short period of time (hours to days) and often found intercalated with sediments in both marine and non-marine realms. The volcanic origin of tephra is often revealed by the presence of primary minerals, including quartz, biotite, zircon, feldspars (commonly sanidine), apatite, monazite, rutile, anatase, and ilmenite (Huff and others, 1996; Huff and others, 1998; Christidis and Huff, 2009; Spears, 2012; Dai and others, 2017). However, in many instances, the primary minerals are altered and the size of fragments decreases with distance from their volcanic source. Because of their metastable nature, volcanic glass and less stable primary minerals in tephra are progressively converted into clay minerals and other secondary products, including zeolites, during alteration. In addition, the abundance, distribution patterns, and ratios of immobile elements such

* UMR CNRS 7285, IC2MP-Department of Geosciences, Université de Poitiers, 86073, Poitiers, France
** COMILOG Society, ERAMET Group, 2728 Moanda, Gabon
§ Laboratoire Magmas et Volcans (Université Clermont-Auvergne-CNRS-IRD-OPGC) 63000, Clermont Ferrand, France
§§ Department of Earth Sciences, University of California, Riverside, California 92521, USA
† Corresponding author: olabode.bankole@univ-poitiers.fr

as Zr, Ta, Nb, Y, and Rare Earth Elements (REE) have been used widely to trace the composition of the parent magma and infer the tectonomagmatic setting of tephra deposits (Huff and Turkmenoğlu, 1981; Clayton and others, 1996; Huff and others, 1996; Huff and others, 1998; Huff, 2008; Christidis and Huff, 2009; Spears, 2012; Huff, 2016; Dai and others, 2017).

Bentonite, which is a common product in altered tephra, consists predominantly of smectite and other minor clay minerals such as kaolinite, illite, and chlorite. Bentonite beds typically range in thickness from a few millimeters to tens of centimeters depending on the distance from their source, which may not be obvious as it could be several hundreds of kilometers away (Huff and others, 1996; Huff, 2016). Bentonite is transformed into K-bentonite during burial diagenesis and low-grade metamorphism by conversion of smectite into illite via mixed-layer illite-smectite (I/S) with the addition of non-exchangeable K^+ ions (for example, Brusewitz, 1988; Christidis and Huff, 2009; Huff, 2016). The resultant illite-rich beds are called K-bentonites or metabentonites because of the introduction of K^+, which is commonly derived from potassium-bearing phyllosilicates including K-feldspar and mica during the illitization process. Smectite and illite are the most important clay minerals in K-bentonites, but significant amounts of kaolinite, chlorite, and zeolites can also be formed depending on the alteration conditions (Huff and others, 1996; Huff, 2016; Dai and others, 2017).

Tephra deposits have been widely used as excellent marker beds for stratigraphic correlation and volcanic-event stratigraphy (Saylor and others, 2005), dating sedimentary sequences and refining chronostratigraphic schemes, especially in non-fossiliferous sequences (Su and others, 2008; Suganuma and others, 2015), and constraining the tectonic and magmatic setting of volcanic rocks (Winchester and Floyd, 1977; Huff and Turkmenoğlu, 1981; Clayton and others, 1996; Huff and others, 1996; Huff and others, 1998; Spears, 2012; Huff, 2016; Dai and others, 2017). Tephra have been formed throughout the whole of Earth history, however, because of their metastable and highly reactive nature, only few occurrences are known from the Precambrian. So far, the oldest reported K-bentonite beds were found in the Mesoproterozoic Belt Supergroup of Montana (Moe and others, 1996) and Xiamaling Formation on North China Craton (Su and others, 2008). Here, we present mineralogy, geochemistry, and zircon age data for the newly-discovered thin, clay-rich K-bentonite beds in the Paleoproterozoic Francevillian Basin with the aim of tracing their mineral evolution, origin, and their implications for the evolution of the Francevillian Basin. Discovery of these K-bentonite beds provides an opportunity to characterize volcanic ash-falls, despite their highly reactive nature, in Paleoproterozoic strata. Their discovery supports the excellent preservation of the Francevillian Basin strata and suggests their deposition in a pro-foreland basin during the early stage of the Nuna (Columbia) supercontinent assembly. These clay-rich K-bentonite beds could thus serve as a potential correlation marker for the Gabonian and adjacent Paleoproterozoic cratons. A K-bentonite of this age is the oldest bentonite deposit that has so far been reported and underlines the continuity and importance of subaerial explosive volcanism in the earlier stage of Earth evolution as well as their preservation potential.

THE FRANCEVILLIAN BASIN

The Francevillian Basin is one of the four sub-basins (fig. 1A) that host the extensive Paleoproterozoic Francevillian Group in southeastern Gabon, and is widely known for its natural nuclear reactor at Oklo (Gauthier-Lafaye, 2006), sediment-hosted manganese deposits (LeClerc and Weber, 1980), and megascopic fossil evidence of multicellular life (El Albani and others, 2010, 2014). The geodynamic setting of the Francevillian Group is not well constrained, but it is likely tied to the break-up of an Archean supercontinent and the subsequent 2.2 to 2.0 Ga Eburnean orogeny that formed the West African Central Belt (WCAB) during the Nuna (Columbia) assembly

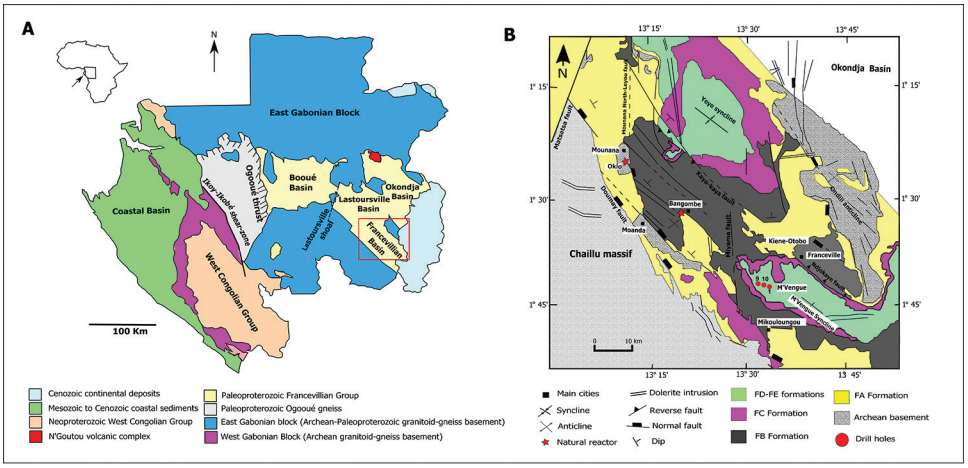

Fig. 1. Geological maps of: (A) Gabon (inset shows Gabon with an arrow on the African continent) and (B) the Paleoproterozoic Francevillian Basin showing locations of the studied drill holes [1 = MVG 1 (1° 43' 46.06" N, 13° 28' 34.57"); 9 = MVG 9 (1° 43' 34.18" N, 13° 28' 13.58"); 10 = MVG 10 (1° 43' 40.62" N, 13° 28' 22.51")].

(Feybesse and others, 1998; Thiéblemont and others, 2009; Weber and others, 2016). Feybesse and others (1998) and Weber and others (2016) attributed the evolution of the Francevillian Group to three main syn-sedimentary tectonic events: (i) rifting and subsequent break-up of an Archean craton, resulting in a shift from continental to marine deposition, (ii) subduction of the eastern craton under the western craton with ocean closure, and (iii) continental collision resulting in the assembly of the Congo craton along the WCAB.

The Paleoproterozoic Francevillian Group is a sequence of 1.0 to 2.5 km-thick unmetamorphosed siliciclastic to volcanoclastic strata that unconformably overlie the Archean crystalline basement of the Chaillu massif, referred to as the East Gabonian block within the Congo craton (fig. 1A; Gauthier-Lafaye and Weber, 1989; Thiéblemont and others, 2009; Weber and others, 2016). The Francevillian Group strata have been divided into five lithostratigraphic formations (FA to FE) in the Francevillian and Okondja basins (figs. 1B and 2; Weber, ms, 1968). The Archean basement is composed of calc-alkaline gneisses, granitoids, and greenstones that were emplaced during two major magmatic events at 2928 to 2870 Ma and 2800 to 2500 Ma (Caen-Vachette and others, 1988; Bouton and others, 2009; Thiéblemont and others, 2009). The FA Formation rests directly on the Archean basement and predominantly consists of fluvial to fluvio-deltaic, coarse- to fine-grained sandstones and conglomeratic sandstones with minor interlayered mudstones (Haubensack, ms, 1981; Gauthier-Lafaye and Weber, 1989; Bankole and others, 2015).

The predominantly marine FB Formation, within which the clay-rich K-bentonite beds are found, has been subdivided into FB1 (a, b, and c) and FB2 (a and b) members based on lithological variations (fig. 2). The FB1a and FB1b units are dominated by fine-grained black shales and siltstones alternating with interbedded medium- to coarse-grained sandstones, breccias, and conglomerates in an upward-fining sequence. The FB1c unit is mainly composed of black shales with interlayered thin iron-rich sediments and a thick manganese ore deposit at the top. The FB2a unit is essentially composed of massive sandstone with thin interlayered black shale observed in few outcrops and it is sharply overlain by the FB2b unit, which is composed of black shales interbedded with thin layers of siltstones. The FB Formation is generally interpreted to

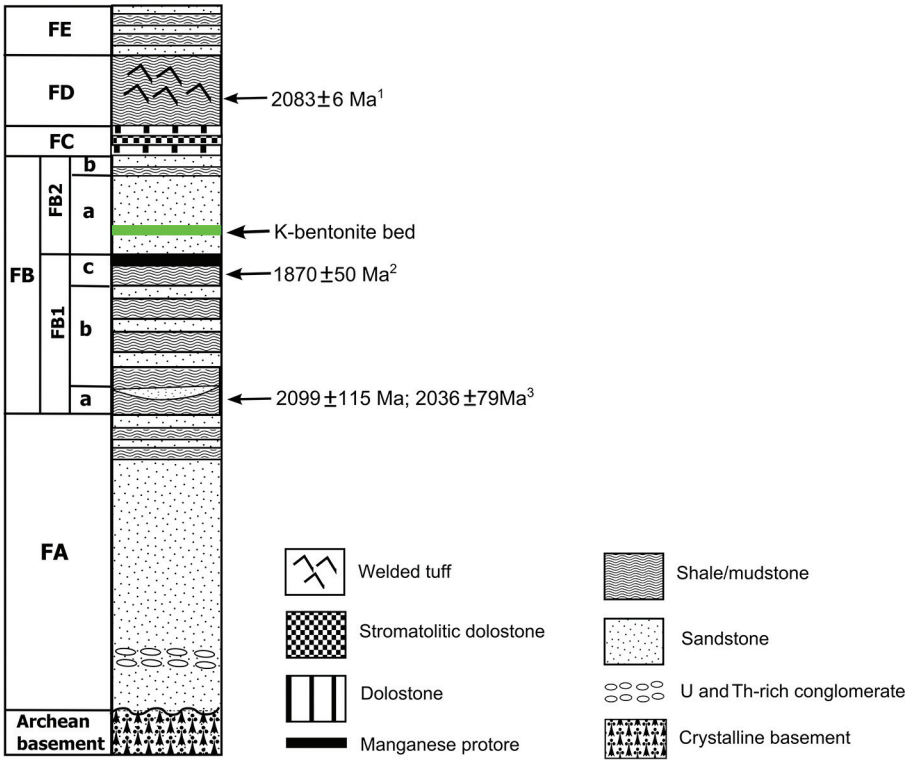

Fig. 2. Lithostratigraphic column of the Francevillian Group showing the stratigraphic position of the K-bentonite beds (modified from Weber, ms, 1968) ([1] Horie and others, 2005; [2] Bonhomme and others, 1982; [3] Bros and others, 1992).

have formed during extension and subsidence in the Francevillian Basin and it is absent in the western Booué Basin. The FB deposition was accompanied by intrusion of alkaline granite and syenite (the N'Goutou Complex), in the northern part of the Okondja Basin (see fig. 1A; Gauthier-Lafaye and Weber, 2003; Thiéblemont and others, 2009, 2014) and emplacement of alkaline volcanic lavas including basalts and trachytes (Thiéblemont and others, 2014) in the basal part of the formation. The overlying FC Formation is a shallow-marine deposit consisting of massive dolostone and thick-banded stromatolitic cherts with thin black shale layers (Weber, ms, 1968; Gauthier-Lafaye and Weber, 2003; Préat and others, 2011). The FD Formation was deposited in a shallow-marine environment and is dominantly composed of black shales with thin, interbedded fine- to medium-grained sandstones and volcanic tuffs throughout the whole formation (Gauthier-Lafaye and Weber, 1989, 2003; Thiéblemont and others, 2009, 2014). The topmost FE Formation consists of epiclastic fine- to medium-grained sandstones with interlayered shales (Gauthier-Lafaye and Weber, 1989, 2003; Thiéblemont and others, 2014). Overall, basin-scale stratigraphic correlation of the Francevillian Group strata appears to be very difficult due to the lateral facies changes and thickness variations and complex tectonic activity during deposition of the Francevillian Group.

Attempts to directly date deposition of the Francevillian Group strata have so far been inconclusive. The timing of early diagenesis in the FB1b unit is constrained by the Sm-Nd isotopic ages of 2099 ± 115 Ma and 2036 ± 79 Ma from the <0.4 μm and <0.2

μm clay fractions, respectively, in the Francevillian Basin (Bros and others, 1992). Dating of <1.5 μm and <2.0 μm authigenic illites from the FB1c unit (fig. 1B) gave an apparent Rb-Sr isochron date of 1870 ± 50 Ma for late diagenesis in the Francevillian Basin (Bonhomme and others, 1982). Horie and others (2005) obtained a SHRIMP U-Pb zircon age of 2083 ± 6 Ma for ignimbrite in the FD Formation; however the data for this age have not yet been published. The N'Goutou Complex that intrudes the FA and FB formations in the Okondja Basin (see fig. 1A) was imprecisely dated at 2027 ± 55 Ma using an upper intercept for discordant TIMS U-Pb zircon data (Moussavou and Edou-Minko, 2006). Consistent with these ages, the FB and FC formations, based on $\delta^{13}C_{carb}$ and $\delta\ ^{13}C_{org}$ trends, are considered to record the end of the 2.22 to 2.06 Ga Lomagundi carbon isotope excursion and to be correlative with the Zaonega Formation in the Onega basin of Karelia, Russia (Kump and others, 2011), which is also imprecisely dated (Ovchinnikova and others, 2007; Martin and others, 2015). The end of the Lomagundi carbon isotope excursion has been bracketed elsewhere in Fennoscandia between 2.11 and 2.06 Ga (Karhu and Holland, 1996; Martin and others, 2013). Combined, these age constraints place the age of deposition for the Francevillian Group close to 2.11 to 2.06 Ga. However, three recent studies challenge this interpretation. First, Martin and others (2015) argued that the Zaonega Formation of Karelia, Russia, which was considered to record the end of the Lomagundi carbon isotope excursion and has been correlated to the FB and FC formations of the Francevillian Group, is much younger at *ca.* 1980 Ma. This interpretation however hinges on the geological position of the dated material, specifically, whether it was derived from a volcanic flow or an intrusive sill, which has not yet been resolved (see Bekker and others, 2016 for further discussion). Secondly, Bekker and others (2016) reported on a short-term, positive C isotope excursion at *ca.* 2.03 Ga. This discovery allows for positive perturbations in the global carbon cycle younger than the Lomagundi carbon isotope excursion. However, available age constraints for the Francevillian Group argue strongly against a *ca.* 2.03 Ga age. Finally, Sawaki and others (2017) published a new MC-ICP-MS ^{207}Pb-^{206}Pb zircon age for the N'Goutou Complex (2191 ± 12 Ma), which, if correct, would shift the depositional age of the Francevillian Group to the beginning of the Lomagundi carbon isotope excursion. However, the authors also recognized the complex nature of the dated zircons and their highly discordant ages. In summary, the age for the end of the Lomagundi carbon isotope excursion, *ca.* 2.11 to 2.06 Ga, currently provides the best estimate for the depositional age of the Francevillian Group.

SAMPLES AND METHODS

Samples.—In this study, seven clay-rich samples from the FB Formation were collected from 3 drill cores near M'Vengue (MVG 1, MVG 9, and MVG 10; figs. 1B and 3A), in the central part of the Francevillian Basin (fig. 1B). These materials are poorly lithified, and occur as sharply bounded, interbedded thin beds with intercalated sandstones and of variable thickness, ranging from <40 cm to ~90 cm (figs. 3A and 3B) in the basal part of the FB2a unit, close to the transition between the FB1c and FB2a units (fig. 2). Two clay-rich beds were identified in the MVG 1 drill-hole, while only one bed was identified in both the MVG 9 and MVG 10 drill cores. Most of the samples are light-green (MVG 1_ 7.2, MVG 1_7.4, MVG 1_7.6, MVG 1_12.5, and MVG 9_ 13), whereas two samples are light red and sandy (MVG 1_ 11.6 and MVG 10_ 35).

Mineralogy and petrography.—The mineralogy of the selected samples was examined by X-ray diffraction (XRD) on bulk powders and clay-size fractions using a Bruker D8 ADVANCE diffractometer (Cu*K*α radiation) with operating conditions of 40 kV, 40 mA, and 0.025/s step size. The powdered bulk-rock samples were examined over the 2°-65° 2θ angular range. For the clay-mineral fractions, the samples were first ultrasonically-dispersed in distilled water to liberate the fine fraction without any chemical treatment.

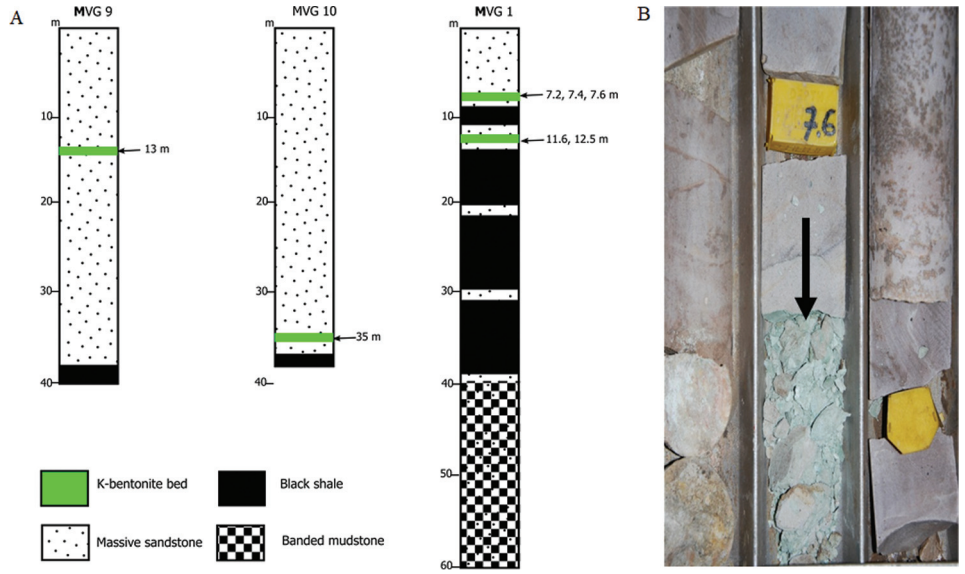

Fig. 3. (A) Schematic log sections of the sampled drill holes showing the stratigraphic positions of the K-bentonite samples; (B) MVG 1 drill hole showing a green K-bentonite bed (black arrow) within sandstones.

The clay-size fraction was separated by sedimentation and program-timed centrifugation (Moore and Reynolds, 1997). Oriented mounts of the <1 μm and <2 μm fractions were prepared by sedimentation on glass slides and analyzed after air-drying overnight at room temperature (AD), ethylene-glycol solvation (EG), and Ca-saturation and heating to 350 °C for 4h. The oriented mounts were scanned from 2° to 35° 2θ angular range for AD and 2° to 30° 2θ for EG and heat treated preparations. Identification of minerals is based on the mineral principal peak positions and comparison with International Centre for Diffraction Data (ICDD) files (Brindley and Brown, 1980; Moore and Reynolds, 1997). Illite polytypes were determined from analysis of the <1 μm and <2 μm random powder mounts from 19° to 34° 2θ angular range. The proportion of the 1M and $2M_1$ illite polytypes was estimated using the method described by Grathoff and Moore (1996). In addition, coarse grains including the heavy mineral fraction were isolated by ultrasonification and sedimentation until clay free. The extracted coarse-grained fraction was analyzed with XRD and scanning electron microscope (SEM). In addition, polished thin sections of samples were prepared parallel and perpendicular to bedding. Thin sections and small sample chips were carbon coated and examined at the University of Poitiers, France with a JEOL JSM 6400 SEM equipped with energy-dispersive detector (EDS), in back-scattered electron (BSE) imaging mode.

Whole-rock geochemistry.—Bulk-rock chemical analyses of four samples were performed on dried and powdered samples at the *Service d'Analyse des Roches et des Minéraux* (SARM-CRPG) in Nancy, France. Major elements were analyzed using inductively-coupled plasma atomic emission spectrometry (ICP-AES) and trace elements, including REE, were analyzed using inductively-coupled plasma mass-spectrometry (ICP-MS).

Zircon dating.—*In situ* U-Pb isotopic data were obtained by laser-ablation inductively coupled plasma spectrometry (LA-ICP-MS) on thin sections at *Laboratoire Magmas & Volcans* in Clermont-Ferrand, France. The analyses involved ablation of zircons with a Resonetics M-50 laser system operating at a wavelength of 193 nm coupled to an

Agilent 7500 cs ICP-MS equipped with a dual pumping system to enhance sensitivity (Paquette and others, 2014). Operational conditions were spot diameter of 15 μm, repetition rate of 3 Hz, and a laser fluence of 4 J/cm^2. The analytical method for isotope dating is similar to that developed and reported by Hurai and others (2010). Data were corrected for U-Pb fractionation occurring during laser ablation and for instrumental mass discrimination by standard bracketing with repeated measurements of the GJ-1 zircon reference material (Jackson and others, 2004). The 91500 zircon reference material (Wiedenbeck and others, 1995) was used as an internal standard. Occurrence of common Pb in the sample was monitored by the evolution of the ^{204}(Pb+Hg) signal intensity, but no common Pb correction was applied owing to the large isobaric interference from Hg. The ^{235}U signal was calculated from ^{238}U on the basis of the ratio ^{238}U/^{235}U = 137.88. Data reduction was carried out with the software package GLITTER® from Macquarie Research Ltd. (van Achterbergh and others, 2001). Calculated isotopic ratios were exported and plotted on a concordia diagram with Isoplot/Ex v. 2.49 (Ludwig, 2001).

RESULTS

Mineral Composition

Detailed mineralogical study has been carried out on the selected samples (figs. 4, 5, 6). Mineralogical data show that the samples are clay-rich and contain a variety of non-clay minerals including quartz, zircon, anatase, biotite, and monazite that are suspended in the clay mineral matrix (figs. 4 and 5). Quartz is the most abundant non-clay mineral, occurring mostly as sub-angular grains of various sizes (fig. 4A). The zircon crystals are generally small (figs. 4B and 4C) with rare larger grains (fig. 4D), sub-rounded to rounded with corroded edges (fig. 4D), and maybe cracked and broken (fig. 4B), suggesting inheritance. Compared to zircon, anatase grains are much smaller in size and occur in lesser amounts (fig. 4C). Biotite occurs as individual elongated brownish flakes (fig. 4E) while the monazite grains are mostly broken and pitted (fig. 4F).

The <1 μm and <2 μm clay-size fraction shows that the samples contain mostly illite and/or mica with associated kaolinite (figs. 6 and A-1). The illite peaks are sharp and do not shift in Ca-saturated slides, but are slightly modified in slides treated with ethylene glycol (EG) and heated to 350 °C (fig. 6). Asymmetric peaks at ~10 Å, typical for illite, indicate the presence of expandable I/S mineral. Decomposed (001) illite peaks in the EG patterns reveal the presence of well-crystallized illite (WCI), poor-crystallized illite, and long-range ordered R3 I/S with ~5 percent expandable layer (figs. 7A, 7B, and A-2). Kaolinite is identified by its 001 and 002 diagnostic peaks at 7.15 Å and 3.57 Å, respectively. Comparison of diagnostic peaks for illite polytypes (Moore and Reynolds, 1997) generated with <1 μm and <2 μm random powder mounts shows that the illite is composed of a mixture of 1M and $2M_1$ illite polytypes (fig. 8). No significant variation in illite polytypes with size fraction was observed in the analyzed samples. The ratios of 1M to $2M_1$ polytypes in the <1 μm fraction are 0.90, 1.20, and 1.98 for the MVG 1_7.2, MVG 9_13, and MVG 10_35 samples, respectively.

Chemical Composition

The SiO_2 content of the K-bentonites ranges from 51.78 to 58.50 percent for the finer MVG 1_7.6 and MVG 9_13 samples and 79.18 to 85.73 percent for the coarser-grained MVG 1_12.5 and MVG 10_35 samples (table 1). SiO_2 inversely varies with Al_2O_3, Fe_2O_3, MgO, TiO_2, and K_2O contents (fig. 9). In contrast, Fe_2O_3, MgO, TiO_2, and K_2O show positive correlation with Al_2O_3 concentration, indicating their control by the abundance of phyllosilicates (clay minerals). The data plot along the illite-kaolinite end-member mixing line on the 4Si-M^+-R^{2+} plot, suggesting that both clay minerals formed during diagenesis and are consistent with a highly illite-rich I/S

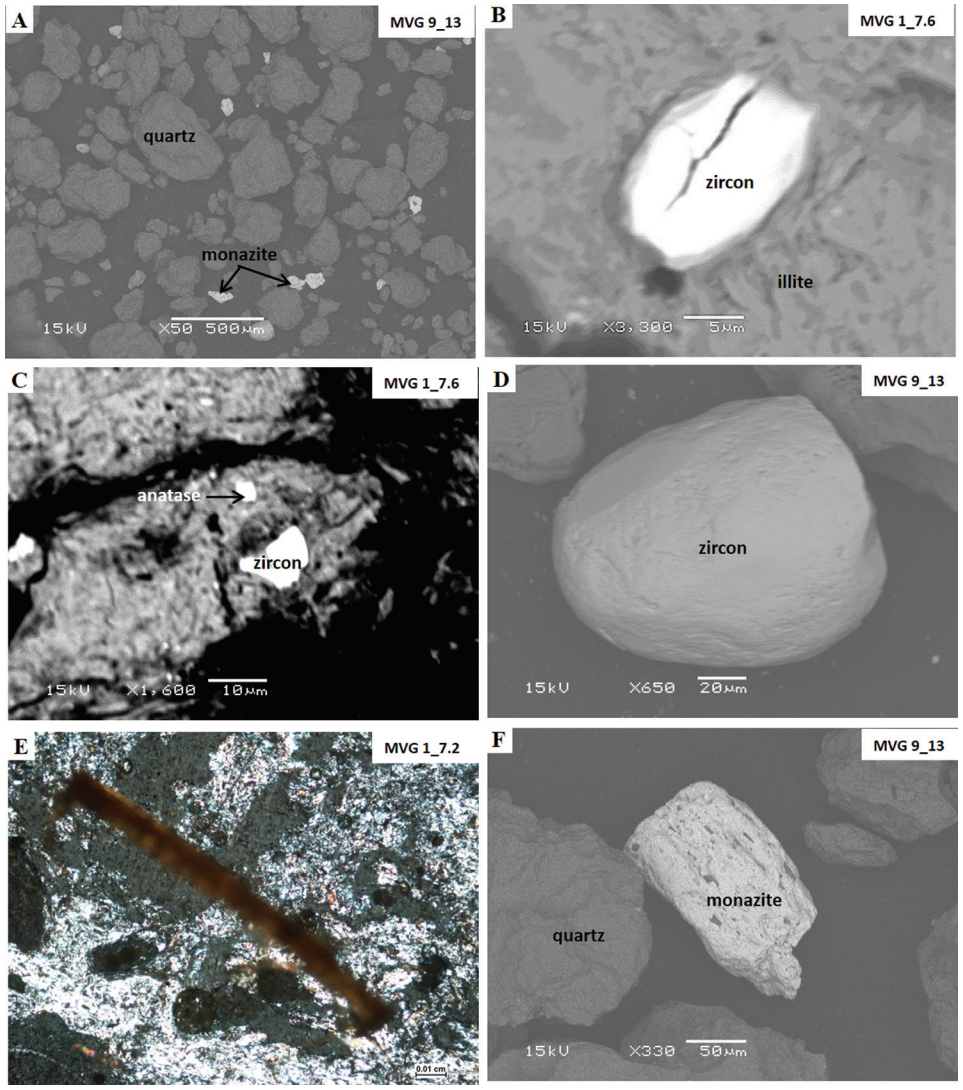

Fig. 4. Micrographs showing examples of the primary mineral grains in the K-bentonite beds of the Paleoproterozoic Francevillian Basin in backscattered scanning electron microscope mode (A, B, C, D, and F) and cross-polarized light (E): (A) quartz and monazite grains in separated coarse-grained fraction; (B) cracked subhedral zircon crystal in illite matrix (thin section); (C) small anatase and zircon crystals in clay mineral matrix (thin section); (D) sub-rounded zircon crystal in separated coarse-grained fraction; (E) elongated, altered biotite grain (thin section); (F) broken and rectangular monazite crystal in separated coarse-grained fraction.

minerals (Meunier and Velde, 2004; fig. 10). CaO and Na_2O are extremely low, ranging from 0.00 to 0.04 and 0.00 to 0.07 percent, respectively, reflecting the absence of carbonates and feldspars.

The trace element and REE data are reported in table 1. All the samples display similar primitive mantle-normalized trace element (fig. 11) and chondrite-normalized REE (fig. 12) patterns. They are characterized by enrichment in large-ion lithophile elements (LILE: Cs, Rb, Ba, and K) relative to the high-field strength elements (HFSEs:

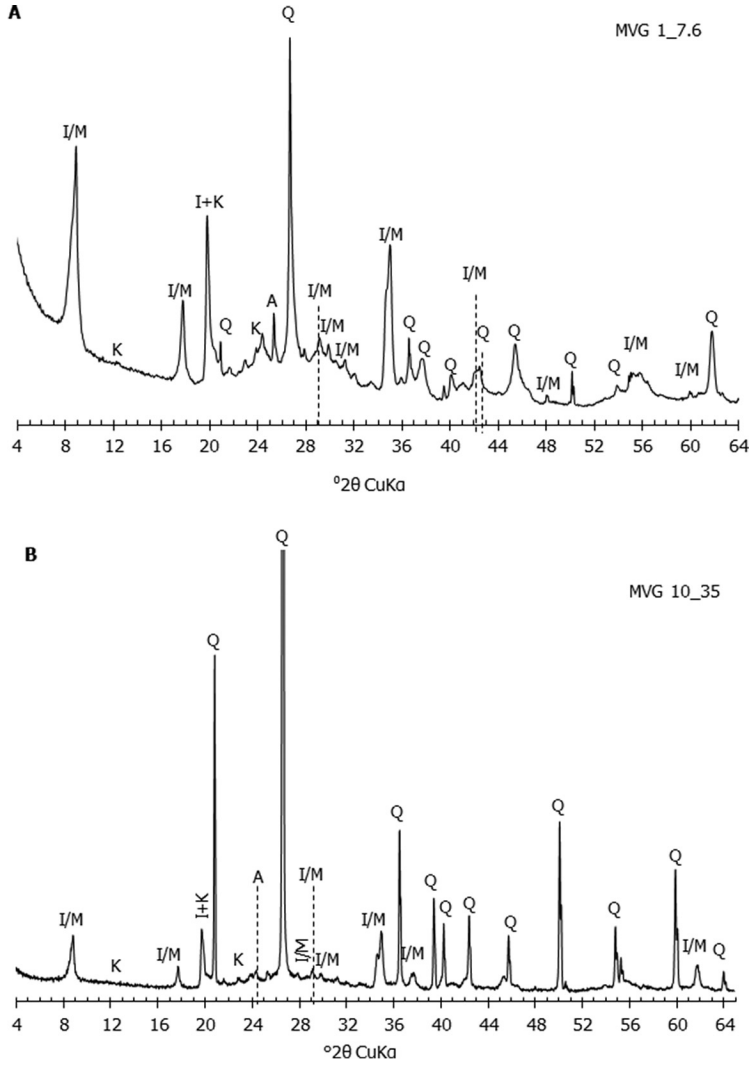

Fig. 5. X-ray diffraction (XRD) patterns of bulk-sample powders of K-bentonites from the Francevillian Basin: (A) MVG 1_7.6; (B) MVG 10_35. I/M = illite/mica; K = kaolinite; Q = quartz; A = anatase.

Y, Zr, Hf, Nb, Ta, and Ti), Ti-Ta-Nb troughs, strongly depleted Sr (fig. 11), and relatively high Th/U ratios between 5.13 and 15.30 (table 1). They all show enrichment in Hf and Zr relative to Ti, indicating the predominance of zircon over Ti-bearing minerals. All samples exhibit REE trends with overall moderate enrichment in light REEs (LREEs) [$(La/Yb)_N$ = 8.69–28.20)], relatively flat heavy REE (HREE) [$(Gd/Yb)_N$ = 1.23–2.85], and weak negative Eu anomalies [$Eu/Eu^* = Eu_N/(Sm_N{*}Gd_N)^{1/2}$ = 0.80–0.89] (fig. 12). REE concentrations decrease with increasing SiO_2 content, reflecting quartz dilution.

U-Pb Zircon Geochronology

U-Pb dates from 31 analytical spots on zircon crystals yield an upper concordia intercept at 2962 ± 16 Ma (fig. 13), omitting 2 outliers. The analyses range from

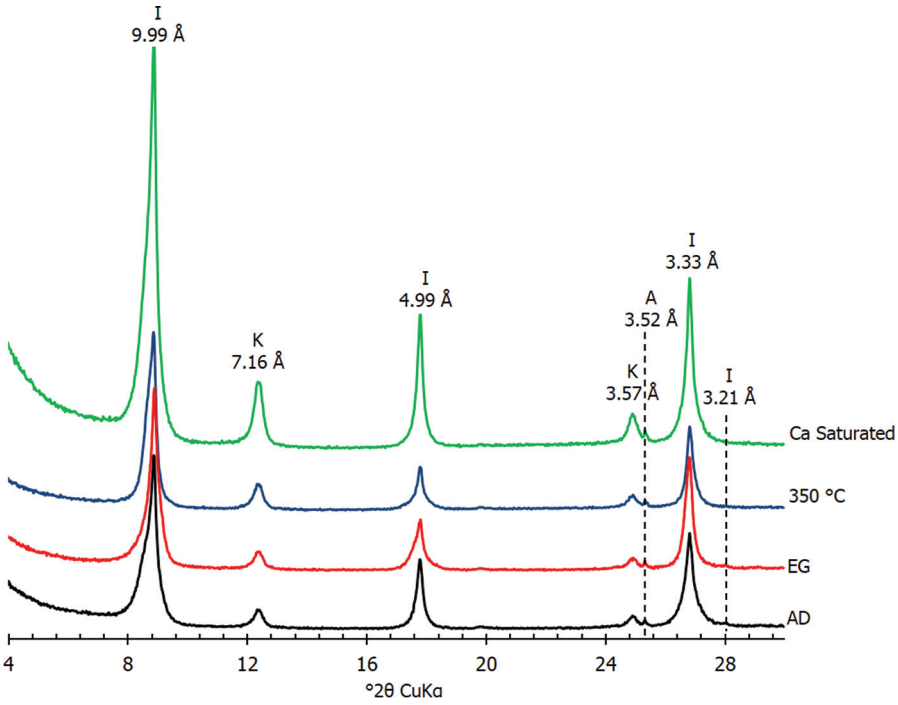

Fig. 6. Representative X-ray diffraction (XRD) patterns of oriented, <2 μm clay fraction in air-dried (AD), ethylene glycol-saturated (EG), heated to 350 °C, and calcium-saturated (Ca-saturated) preparations for the sample MVG 1_7.2. I = illite; K = kaolinite; Q = quartz; A = anatase.

concordant to 83 percent discordant with the most discordant grains displaying the highest U and Th contents. The $^{207}Pb/^{206}Pb$ ages are consistent with a weighted mean of 2971 ± 13 Ma (MSWD = 1.0). We interpret the zircon crystallization age as 2962 ± 16 Ma. Their variable Th/U ratios between 0.3 and 4.9 (table 2), with a relatively high mean value of 1.78, are indicative of a magmatic origin and not the result of metamorphic overprinting (Paquette and Mergoil-Daniel, 2009; Hurai and others, 2010). Given the discordia passes close to the origin, the Pb loss and high contents of U and Th of the *ca.* 3 Ga zircons (contributing over a long time to the metamictization of zircon lattice) likely suggests a recent event that is related to fluid ingress.

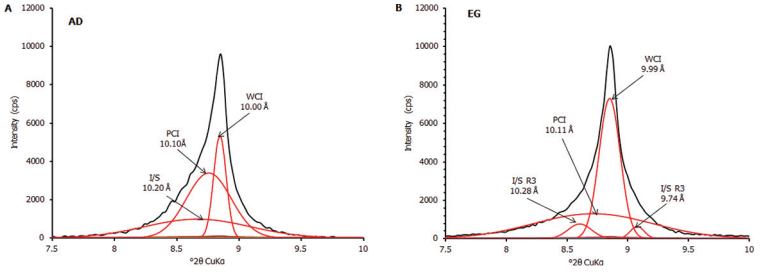

Fig. 7. Decomposed 001 illite peaks of <1 μm clay fraction in (A) air-dried (AD) and (B) ethylene glycolated (EG) preparations for sample MVG 9_13. WCI = well-crystallized illite; PCI = poorly crystallized illite; I-S = illite-smectite mixed-layer clay minerals.

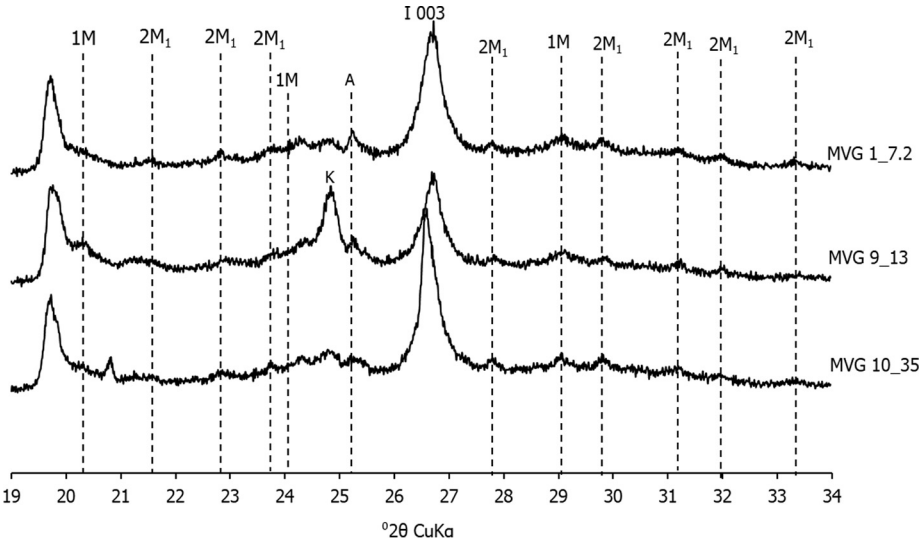

Fig. 8. XRD patterns of <1 μm random powder showing signature of illite polytypes in 3 samples of the M'Vengue K-bentonites, Francevillian Basin, Gabon. I = illite; 1M and 2M1 = illite polytypes; A = anatase; K = kaolinite.

DISCUSSION

Mineralogy

Mineralogy and chemical composition of the olive-green to light-red, clay-rich thin beds within the FB2 member of the Francevillian Basin demonstrate that they are K-bentonites. They have sharp contacts with the basal sandstones, suggesting rapid change in the depositional environment. The predominance of illite, trace amounts of mixed-layer I/S minerals, significant amounts of kaolinite, and the nature of illite polytypes are all characteristic of K-bentonites formed by kinetically controlled, prolonged smectite illitization at low temperature (Velde and Vasseur, 1992). The absence of smectite in the samples does not imply that it was never present, but rather reflects an advanced stage of smectite illitization. K-feldspar, which is the main source of K^+ for smectite illitization process, is completely absent in the studied samples, suggesting diffusion of potassium derived from dissolution of K-bearing minerals in adjacent lithologies into the bentonites (Huff and Turkmenoğlu, 1981; Brusewitz, 1988; Stille and others, 1993). Considering the age of the Francevillian Group, one would expect the predominance of $2M_1$ over 1M polytype in such old rocks, but our observations suggest otherwise as 1M polytype appears to be as abundant as $2M_1$ polytype in the K-bentonites (fig. 8). Therefore, the coexistence in equal amounts of $2M_1$ and 1M illite polytypes, which are the ultimate products of smectite alteration in diagenetic smectite-to-illite reaction, cannot be explained by low-grade metamorphic conditions or inheritance of detrital mica, but rather indicates prolonged recrystallization, which is consistent with the age of the succession. Kaolinite in altered volcanic ash is mainly an authigenic product of altered biotite, feldspars, amphiboles, and pyroxenes (Dai and others, 2017). Kaolinite is unstable at higher diagenetic temperatures where it is replaced by either illite or chlorite. Although, we could not identify the precursor mineral for kaolinite in this study, its preservation in substantial amounts in the Francevillian Basin K-bentonites constrains the alteration process to relatively low temperatures and shallow depths.

TABLE 1

Bulk major and trace element compositions of four K-bentonite samples from the Francevillian Basin, Gabon

Sample	MVG1_7.6	MVG 9_13	MVG 10_35	MVG 1_12.5
Major elements (%)				
S_2	51iO.78	58.50	85.73	79.18
Al_2O_3	28.76	25.46	7.83	12.54
Fe_2O_3	0.88	0.59	0.39	0.36
MnO	0.00	N.D.†	N.D.†	N.D.†
MgO	1.83	1.14	0.49	0.85
CaO	0.04	N.D.†	N.D.†	N.D.†
Na_2O	0.07	0.04	N.D.	N.D.
K_2O	8.62	5.82	2.37	3.36
TiO_2	0.72	0.63	0.13	0.43
P_2O_5	0.11	N.D.†	N.D.†	N.D.†
LOI*	6.53	6.62	1.84	3.31
Total	99.35	98.79	98.78	100.3
Trace elements (ppm)				
As	N.D.†	4.31	0.47	0.22
Ba	1739	1470.85	630.87	715.40
Be	2.547	1.53	0.43	1.14
Bi	0.5	0.26	0.18	0.20
Cd	0.33	0.26	0.04	0.06
Ce	141.2	67.47	9.91	96.93
Co	1.51	1.09	0.38	0.45
Cr	3302	3359.61	46.85	62.37
Cs	11.14	3.61	1.50	4.32
Cu	17.72	8.71	N.D.†	N.D.†
Dy	4.57	2.12	0.43	2.63
Er	2.04	1.36	0.34	1.42
Eu	2.10	0.88	0.12	1.25
Ga	39.55	20.43	8.96	15.77
Gd	6.94	2.54	0.35	3.85
Ge	1.57	1.23	0.72	1.02
Hf	11.8	19.01	2.84	6.17
Ho	0.76	0.45	0.11	0.52
In	0.11	0.04	0.02	0.03
La	71.43	45.32	4.91	54.31
Lu	0.30	0.25	0.06	0.20
Mo	N.D.†	N.D.†	N.D.†	N.D.†
Nb	11.14	8.99	1.82	6.46
Nd	55.38	31.10	3.46	34.73
Ni	27.08	23.15	11.24	11.94
Pb	18.87	5.07	1.15	33.75
Pr	15.44	9.08	0.98	10.12
Rb	218.9	144.41	52.70	88.93
Sc	11.81	11.67	3.07	5.39
Sb	0.248	0.20	0.15	0.12
Sm	9.266	4.18	0.51	5.26
Sn	1.9	N.D.†	N.D.†	N.D.†
Sr	92.72	19.14	2.42	25.58
Ta	0.97	0.75	0.16	0.55
Tb	0.90	0.35	0.06	0.48
Th	26.72	15.02	3.34	13.45
Tm	0.30	0.22	0.05	0.20
U	1.75	2.92	0.33	2.55
V	131.8	65.91	22.99	45.28
W	20.98	13.77	1.95	2.24
Y	24.51	13.28	3.86	17.64
Yb	1.96	1.61	0.38	1.31
Zn	55.03	37.62	8.98	13.79

Note: * LOI = Loss on ignition; † N.D. = not detected.

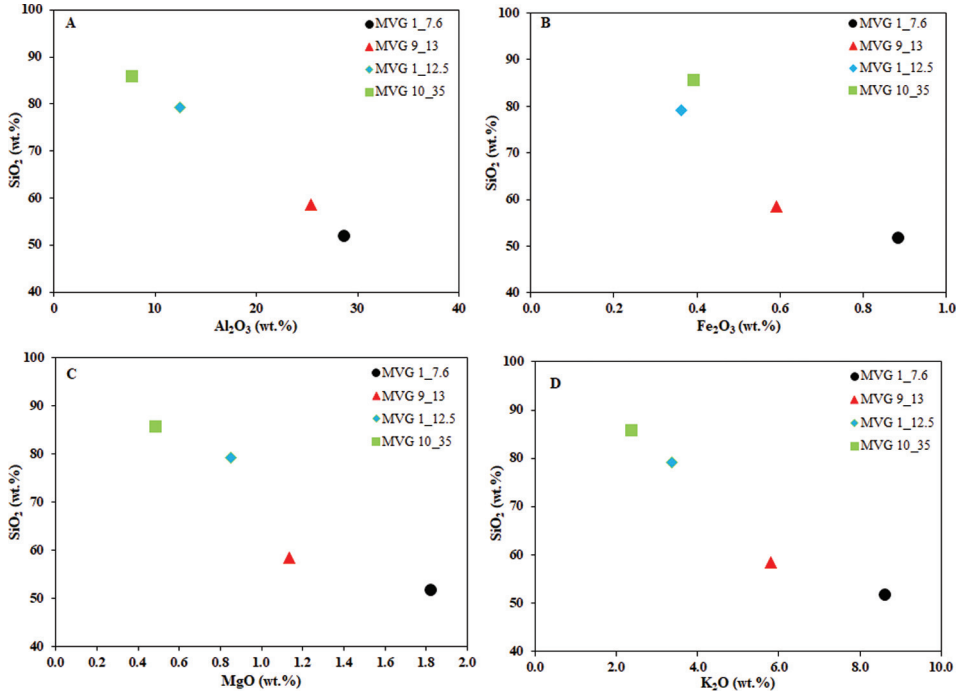

Fig. 9. Whole-rock elemental bivariate plots of SiO_2 versus selected major element oxides for the K-bentonites from the Paleoproterozoic Francevillian Basin, Gabon: (A) SiO_2 vs. Al_2O_3; (B) SiO_2 vs. Fe_2O_3; (C) SiO_2 vs. MgO; (D) SiO_2 vs. K_2O.

Clay mineralogy of the K-bentonites is similar to that of the other described Precambrian K-bentonites (Moe and others, 1996) and is remarkably different from that of the surrounding FB Formation shales and sandstones. The FB2b and FB1c units black shales and sandstones contain randomly and regularly ordered I/S minerals, chlorite, $1M_d/1M_1$ illite polytypes, and non-clay minerals including quartz, plagioclase, muscovite, pyrite, and dolomite (Bros and others, 1992; Ossa Ossa and others, 2013; Ngombi-Pemba and others, 2014). Notably, these are the only known Precambrian shales with preserved smectite-rich, randomly ordered I/S minerals. Ossa Ossa and others (2013) attributed survival of I/S minerals to sluggish illitization in the presence of abundant organic matter; Ngombi-Pemba and others (2014) argued that their presence was due to incomplete illitization related to low-K content of the FB Formation lithologies. We consider that the difference in mineral composition between the K-bentonites and adjacent shales likely reflects different source composition, depositional conditions, and, consequently, post-depositional alteration pathways.

Spears (2012) suggested that small rounded to sub-rounded zircon grains in volcanic ash are due to either magmatic processes before ash eruption or to transport in the ash cloud, while studies such as by Guerra-Sommer and others (2008) and Huff and others (1997) proposed that large rounded zircon grains in volcanic ash indicate inheritance from the basement. Zircon grains in the Francevillian Basin K-bentonites vary in size and are mostly rounded with the ages similar to those of the underlying Mesoarchean calc-alkaline granitoids (2928 ± 6 Ma; Thiéblemont and others, 2009), and older than the constrained depositional age of the FB Formation where they are found. Combined, these observations clearly indicate that these zircons did not

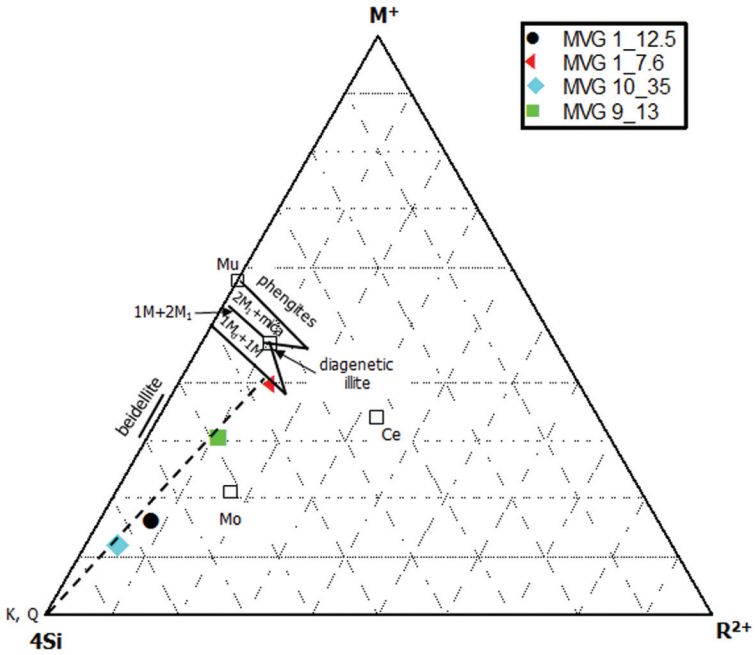

Fig. 10. Projection of the bulk geochemical composition of the M'Vengue K-bentonites from the Francevillian Basin, Gabon on the 4Si-M^{+}-R^{2+} ternary plot (after Meunier and Velde, 2004). The Francevillian K-bentonites plot along the dashed line with kaolinite and diagenetic illite end-members, which indicates the presence of illite-rich, I/S mixed-layer clay-minerals. The calculated half-unit structural formula of the diagenetic illite is $(Si_{3.45}Al_{0.55})(Al_{1.71}Fe_{0.04}Mg_{0.18}Ti_{0.03})O_{10}(OH)_2K_{0.73}Na_{0.01}$. Mu = muscovite; Ce = celadonite; Mo = montmorillonite; K = kaolinite; Q = quartz.

crystallize from the magma, but are older, inherited zircons from either the Archean basement granitoids or older clastic sediments and incorporated into the magma during magmatic activity that produced the Francevillian Basin tephra.

Geochemistry and Geochronology

Owing to the susceptibility of the major elements to alteration processes, they cannot be used to investigate the composition of the original magma. However, incompatible trace elements such as Nb, Ta, Ti, Th, Y, Zr, and REEs have been widely used to provide geochemical information on the altered tephra and tectonic setting of the volcanic source (Huff and Turkmenoğlu, 1981; Clayton and others, 1996; Huff and others, 1996; Huff and others, 1998; Christidis and Huff, 2009; Spears, 2012; Huff, 2016; Dai and others, 2017). This is based on the assumption that they are the least affected and least mobile under conditions of low-temperature sedimentary processes (transport, weathering, and diagenesis), low-grade metamorphism, and devitrification of volcanic glass to clay (for example, Winchester and Floyd, 1977; Pearce and others, 1984; Batchelor and Jeppsson, 1994; Huff and others, 1996; Huff and others, 1998; Huff, 2016). The geochemical behavior of these elements depends on the original host phases (volcanic glass or igneous mineral) and the mechanism of alteration. Depletion of Nb and Ta relative to the primitive mantle, moderate enrichments of LILE and LREE, depletion of HFSE and HREE, weak negative Eu anomalies, and low concentrations of REE displayed by the K-bentonites are all characteristic of subduction-related intermediate to felsic calc-alkaline magmas in a continental-arc setting (figs. 11 and 12; Taylor and McLennan, 1985; Huff and others, 1998; Lustrino and Wilson, 2007).

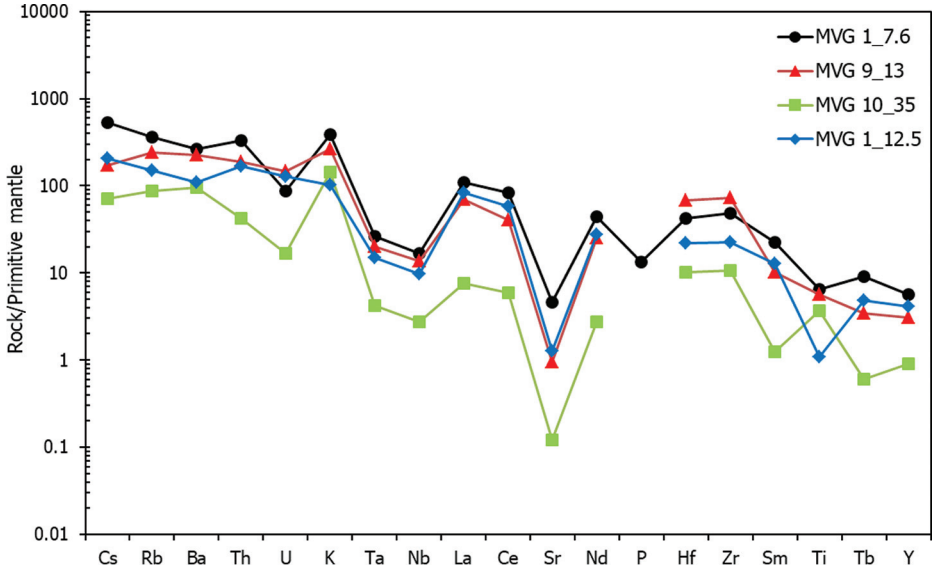

Fig. 11. Primitive mantle-normalized trace-element patterns of the K-bentonites from the Paleoproterozoic Francevillian Basin, Gabon. Phosphorus (P) content in most of the sample is 0. Data for the primitive mantle are from McDonough and Sun, 1995.

Unlike the geochemistry of juvenile, undifferentiated volcanic arcs, enriched LREE, weak negative Eu anomalies, and, in particular, low Th/U ratios of the K-bentonites indicate contribution from a less evolved continental crust (McLennan and others,

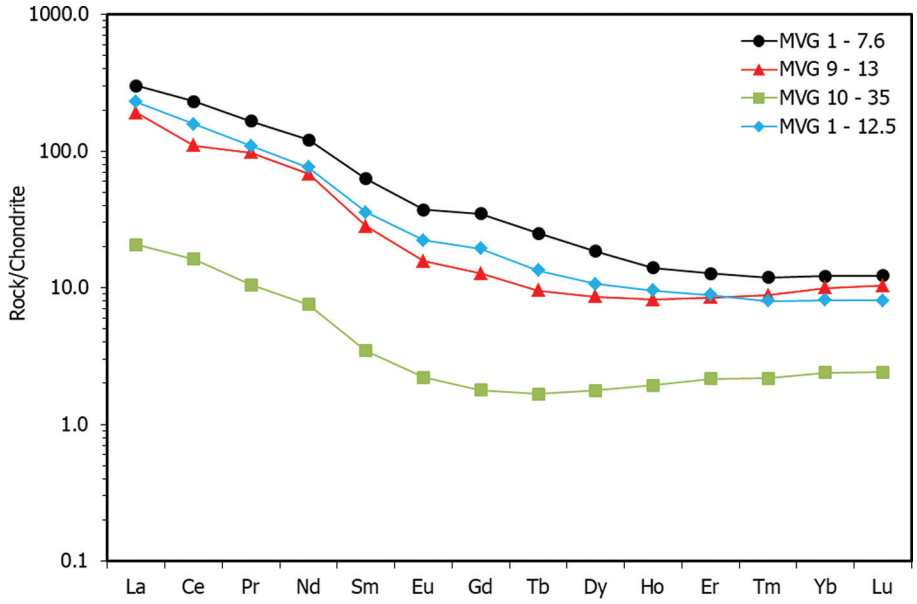

Fig. 12. Chondrite-normalized REE patterns for K-bentonites from the Paleoproterozoic Francevillian Basin, Gabon. Chondrite data are taken from McDonough and Sun (1995).

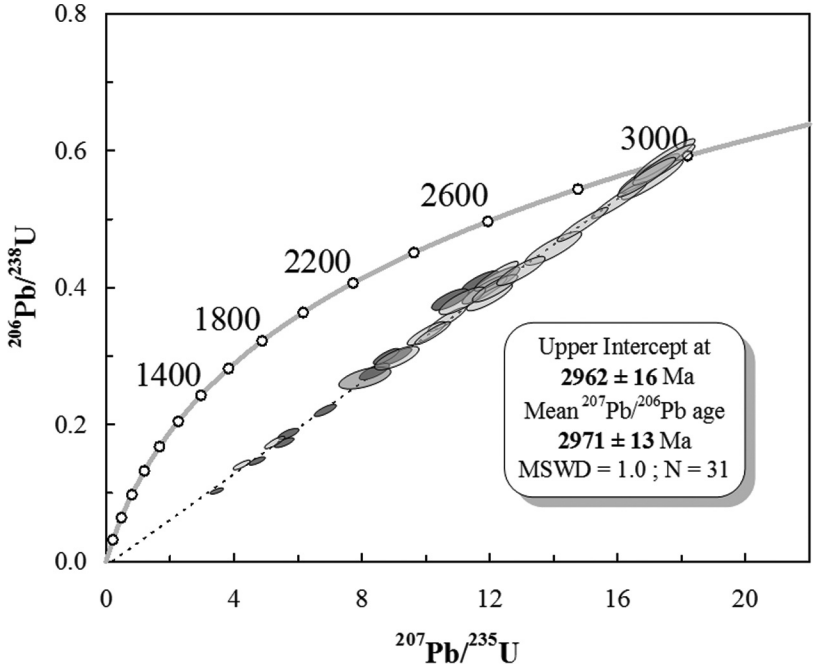

Fig. 13. U-Pb concordia diagram for dated zircons in sample MVG1_7.6. Computed $^{207}Pb/^{206}Pb$ ages are given with 2σ errors. The dark-gray and light-gray shades of ellipses correspond to thin sections prepared parallel and perpendicular to the bedding, respectively. MSWD = mean square of weighted deviates.

1993), favoring intermediate magma composition. Weak negative Eu anomalies could also suggest the following: feldspar was not the main fractionating phase in the melt; oxygen fugacity of the melt was high (Batchelor and Jeppsson, 1994; Huff and others, 1998); incomplete plagioclase crystallization; and intermediate composition of the magma (Huff and others, 1998). In contrast, the pronounced Sr depletion with respect to the primitive mantle, which is shown by all K-bentonite samples, might reflect Sr mobility in fluids during diagenesis (Huff and others, 1998; Kiipli and others, 2010; Huff, 2016).

Discriminant diagrams based on ratios of immobile elements have been applied to provide additional information on the tectonic setting and magma composition of altered volcanic ash. Numerous studies (for example, Huff and Turkmenoğlu, 1981; Clayton and others, 1996; Huff and others, 1996; Huff and others, 1998; Spears, 2012; Dai and others, 2017) applied the Zr/TiO_2 vs. Nb/Y plot (originally proposed by Winchester and Floyd, 1977) to assess geochemical fingerprints of the tephra source magma, where Zr/TiO_2 ratio is used as an index of magma differentiation and Nb/Y ratio as a measure of alkalinity. However, this discriminant diagram cannot be applied in this study because most of the zircon crystals were inherited and are not representative of the primary magma that produced the tephra. Pearce and others (1984) used immobile trace elements, Nb and Y, to distinguish between within-plate volcanism and that produced in arcs, and Ta and Yb to further separate volcanic-arc granite (VAG) from syn-collisional granites. Orogenic setting for the magmatic system from which the Francevillian Basin K-bentonites were derived can be evaluated using the Nb vs. Y (fig. 14A) and Ta vs. Yb (fig. 14B) diagrams, where the Francevillian Basin K-bentonite plots in the VAG field. These diagrams suggest that magmatism took place in a continental

TABLE 2

Zircon U-Pb data for the MVG 1_7.6 K-bentonite obtained by in situ laser ablation MC-ICP-MS

Spot	Pb* (ppm)	Th* (ppm)	U* (ppm)	Th/U	$^{207}Pb^{2}/^{235}U$	$^{207}Pb/^{235}U$ 2σ error	$^{206}Pb^{2}/^{238}U$	$^{206}Pb/^{238}U$ 2σ error	$^{207}Pb/^{206}Pb$	$^{207}Pb/^{206}Pb$ 2σ error	Rho	$^{207}Pb/^{206}Pb$ Age (Ma)	$^{207}Pb/^{206}Pb$ 2σ error
Perpendicular to bedding													
1	128	348	335	1.04	9.074	0.358	0.300	0.010	0.219	0.006	0.83	2976	64
2	12	46	34	1.33	8.327	0.387	0.278	0.010	0.217	0.007	0.75	2961	77
3	112	147	240	0.61	11.894	0.416	0.400	0.012	0.215	0.005	0.89	2946	56
4	64	377	228	1.65	6.794	0.281	0.221	0.007	0.223	0.006	0.80	3004	68
5	82	697	351	1.98	5.653	0.266	0.187	0.006	0.220	0.007	0.74	2979	78
6	8	47	19	2.42	8.046	0.658	0.268	0.013	0.218	0.013	0.59	2964	138
7	42	258	110	2.35	8.707	0.338	0.300	0.010	0.210	0.006	0.82	2909	63
8	28	385	122	3.16	5.520	0.251	0.174	0.006	0.230	0.007	0.75	3052	75
9	51	1035	385	2.69	3.388	0.166	0.103	0.004	0.238	0.008	0.72	3107	81
10	59	528	296	1.78	4.661	0.202	0.147	0.005	0.230	0.007	0.76	3055	71
11	38	156	75	2.08	11.671	0.483	0.409	0.013	0.207	0.006	0.78	2883	68
12	30	121	64	1.89	10.723	0.474	0.383	0.013	0.203	0.006	0.75	2850	73
Parallel to bedding													
13	55	29	85	0.34	17.071	0.788	0.557	0.024	0.222	0.005	0.92	2997	69
14	39	21	60	0.34	16.987	0.771	0.566	0.024	0.218	0.005	0.93	2963	68
15	47	61	74	0.83	16.036	0.718	0.527	0.022	0.221	0.005	0.94	2985	67
16	42	22	62	0.36	17.464	0.791	0.586	0.025	0.216	0.005	0.93	2951	68
17	48	83	88	0.94	13.971	0.725	0.457	0.020	0.222	0.006	0.85	2995	80
18	33	18	49	0.36	17.441	0.798	0.579	0.024	0.219	0.005	0.92	2970	69
19	62	79	109	0.73	14.884	0.657	0.492	0.021	0.220	0.005	0.94	2977	66
20	58	31	89	0.35	16.892	0.752	0.561	0.023	0.218	0.005	0.94	2969	67
21	40	150	81	1.85	12.153	0.623	0.408	0.018	0.216	0.006	0.86	2950	80
22	39	80	84	0.95	11.823	0.575	0.396	0.017	0.216	0.005	0.88	2954	75
23	8	84	20	4.19	9.057	0.570	0.296	0.014	0.222	0.008	0.75	2994	101
24	34	127	70	1.81	12.172	0.567	0.416	0.018	0.212	0.005	0.90	2922	71
25	94	239	200	1.20	10.632	0.486	0.353	0.015	0.219	0.005	0.91	2971	70
26	35	170	84	2.02	9.978	0.488	0.333	0.014	0.218	0.006	0.86	2963	76
27	133	467	306	1.52	10.182	0.458	0.333	0.014	0.222	0.005	0.91	2994	69
28	56	300	108	2.79	11.961	0.591	0.385	0.016	0.225	0.006	0.85	3017	77
29	31	210	63	3.31	11.110	0.589	0.380	0.016	0.212	0.006	0.82	2920	84
30	82	2129	436	4.88	4.190	0.214	0.140	0.006	0.217	0.006	0.83	2959	81
31	79	1497	351	4.26	5.222	0.257	0.173	0.007	0.219	0.006	0.85	2971	78
32	88	242	175	1.39	12.129	0.585	0.398	0.017	0.221	0.006	0.86	2987	75
33	89	226	167	1.35	12.952	0.620	0.423	0.018	0.222	0.006	0.86	2994	75

Note: * Concentration uncertainty ~20%; † Uncorrected data for non-radiogenic or common Pb; § Error correlation coefficient for $^{207}Pb/^{204}Pb$-$^{206}Pb/^{204}Pb$.

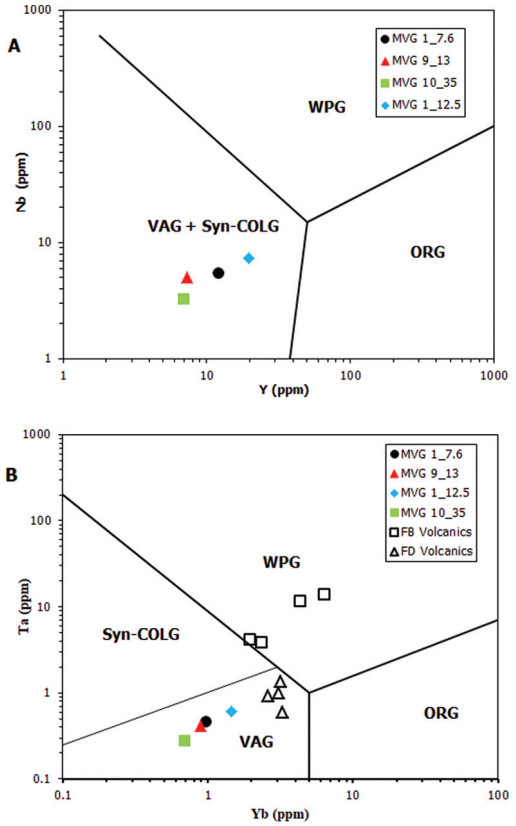

Fig. 14. The Francevillian Basin K-bentonite data plotted on the granite discrimination diagrams of Pearce and others (1984). (A) Nb versus Y; (B) Ta versus Yb. All values were normalized to Al_2O_3 ([14/Al_2O_3] x elemental concentration) to account for residual elemental enrichment during diagenesis (Kiipli and others, 2010). Data for volcanics in the FB and FD formations are from Thiéblemont and others (2014). WPG = within-plate granite; ORG = ocean-ridge granite; VAG = volcanic-arc granite; syn-COLG = syn-collisional granite.

arc setting and involved partial melting of the continental crust (Pearce and others, 1984; Huff, 2016).

All the zircons in our samples show the age of the Archean basement. Although this is an unusual case, it is possible that only inherited zircons are present, especially when the magma is of intermediate to felsic composition and similar observations have previously been reported in the literature. For example, Bea and others (2007) documented that most of the zircons in the metavolcanic rocks of Central Iberia are older than the host volcanic rocks. Survival of such inherited zircons was attributed to rapid melt generation, fast magma transfer and cooling at the surface, low magma temperatures to melt zircons, and/or kinetic effects that hindered their melting. Inherited zircons from host rocks or underlying siliciclastic sediments have been documented in multiple studies of felsic volcanic tuffs (Huff and others, 1998; Batchelor and Jeppson, 1999; Spears, 2012; Dai and others, 2017). Pickard (2002, 2003) has shown that both felsic and mafic tuffs associated with the Paleoproterozoic iron formations in the Hamersley Province of Western Australia and Transvaal Basin of South Africa contain inherited zircons re-sedimented from the underlying sedimentary units. We conclude that absence of zircons with Paleoproterozoic ages in the

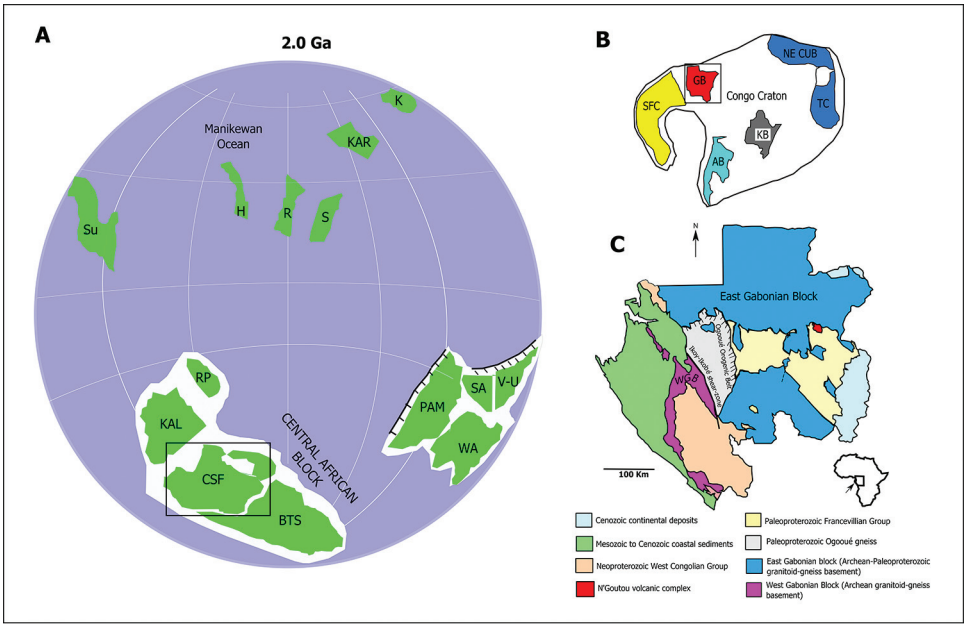

Fig. 15. Paleogeographic reconstructions showing position of the Francevillian Basin within the assembling Nuna (Columbia) supercontinent during the Paleoproterozoic: (A) paleogeographic position of South American and African cratons at *ca.* 2.0 Ga during the Nuna (Columbia) supercontinent assembly (modified from D'Agrella-Filho and others, 2016; D'Agrella-Filho and Cordani, 2017; abbreviations for the shown cratons: Su = Superior; H = Hearne; R = Rae; S = Slave; KAR = Karelia; K = Kola; RP = Rio de la Plata; KAL = Kalahari; CSF = Congo/São Francisco; BTS = Borborema/Trans-Sahara; PAM = Proto-Amazon; WA = West Africa; SA = Sarmatia; V-U = Volgo-Uralia); (B) The Congo-São Francisco cratons (marked by the rectangle in A and rotated 90° anticlockwise in B) showing the Gabon blocks (marked with the rectangle) and other African blocks within the Congo craton (modified from Fernandez-Alonso and others, 2012; abbreviations: SFC = São Francisco Craton; GB = Gabon Blocks; NE CUB = North-East Congo-Uganda Blocks; TC = Tanzania Craton; KB = Kasal Block; AB = Angola Block); (C) Tectonic map of Gabon showing the West and East Gabonese blocks, the Ogooué Orogenic Belt, N'Goutou Complex, and the Francevillian and other sub-basins where the Francevillian Group is developed (modified from Thieblemont and others, 2014; WGB = West Gabonian Block).

Francevillian Basin K-bentonites is due to the intermediate magma composition that reflects rapid melt generation, transfer, and cooling in a continental arc setting.

Implications for Evolution of the Francevillian Group

Earlier studies established that magmatism during deposition of the Francevillian Group resulted in the emplacement of the N'Goutou Complex into the FA and FB formations in the Okondja Basin and deposition of the FD tuffs (Thiéblemont and others, 2014; Weber and others, 2016). These volcanic events were interpreted to record a change from alkaline magmatism of ultramafic and trachytic composition during deposition of the FB Formation to calc-alkaline magmatism of felsic composition during deposition of the FD Formation. The transition from alkaline to calc-alkaline magmatism was linked to a change from a within-plate, rift-related to a subduction-related setting (Thiéblemont and others, 2014; Weber and others, 2016; fig. 14B), leading to a continental collision between the West Congolian and São Francisco cratons that resulted in the Central African Eburnean Orogenic Belt (fig. 15). In Gabon, the East Gabonian block contains the Paleoproterozoic Ogooué fold-and-thrust belt in its western part, while the West Gabonian block hosts 2.08 to 2.04 Ga K-granitoids, emplaced during west-directed subduction of oceanic crust that

separated these blocks (Thiéblemont and others, 2009; Weber and others, 2016). Geochemical similarity of the FB2 member K-bentonites and FD Formation volcanics suggests a similar magmatic source and geodynamic setting despite the difference in their stratigraphic position and mineral composition (fig. 14B; see Thiéblemont and others, 2009). We thus infer that the K-bentonites in the FB Formation were also derived from continental arc volcanoes of the West Gabonian block, implying that the Francevillian Basin developed proximally to the approaching continental arc in a pro-foreland basin typically characterized by a short lifespan and high sedimentation rates (Sinclair and Naylor, 2012). Excellent preservation of lithologies in the Francevillian Basin, recognized both previously (for example, Ossa Ossa and others, 2013; Ngombi-Pemba and others, 2014; Bankole and others, 2015, 2016) and in this study, likely reflects deposition in a distal part of the pro-foreland basin developed in the core of the Nuna (Columbia) supercontinent during the early stage of its assembly (fig. 15).

CONCLUSIONS

Sedimentary textures, mineralogy, and chemical composition demonstrate the bentonite nature of the olive-green to light-red thin beds in the *ca.* 2.1 Ga Francevillian Basin, Gabon. Their clay mineral composition suggests a diagenetic origin via smectite to illite transformation over a prolonged period of time at low temperature. The chemical composition of the FB2 member K-bentonite beds suggests derivation from intermediate to felsic magma with a calc-alkaline affinity similar to that of the stratigraphically higher FD Formation volcanics and is consistent with proximity to the continental arc developed on the West Gabonian block. We infer that the Francevillian Basin was developed in a pro-foreland setting characterized by a short lifespan and high sedimentation rates. The zircon shapes and U-Pb zircon dates from the K-bentonite suggest inheritance from the Archean basement during magmatic activity. These K-bentonites are the oldest bentonites that have been so far reported and their deposition as well as preservation likely reflects initiation of the Nuna (Columbia) supercontinent assembly that subsequently locked this basin in the core of the supercontinent (fig. 15). These K-bentonites could thus serve as a potential stratigraphic correlation marker for the Gabonian and adjacent cratons at *ca.* 2.1 Ga.

ACKNOWLEDGMENTS

This study was supported by CNRS-INSU, FEDER, the University of Poitiers, Nouvelle Aquitaine Region, and the French Embassy Libreville, Gabon. We warmly thank the Gabonese Government, CENAREST, General Direction of Mines and Geology, *Agence Nationale des Parcs Nationaux* of Gabon for logistic supports. We thank COMILOG Gabon for providing the core samples and permission to access their core sample facilities. We are grateful to Prof. P. Mouguiama Daouda for his support during the fieldtrip. We also acknowledge C. Fontaine, C. Laforest, and N. Dauger for laboratory support at the University of Poitiers. We greatly appreciate edits, comments, and suggestions provided by reviewers of this and previous versions of the paper: Warren Huff, Richard Batchelor, George Christidis, Elisa Fitz-Diaz, Francois Gauthier-Lafaye, Robert Pankhurst, and Tony Prave. We are particularly thankful to the Associate Editor Simon Wilde for his careful editing.

APPENDIX

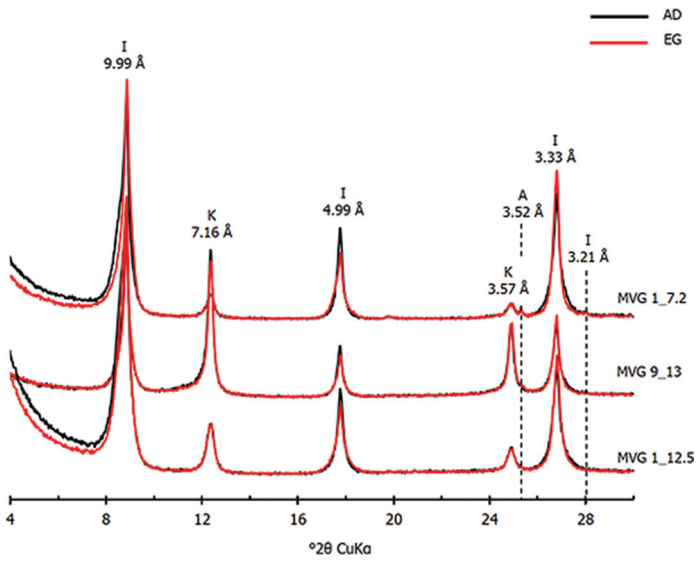

Fig. A-1. X-ray diffraction (XRD) patterns of oriented <2 μm clay fraction in air-dried (AD) and ethylene glycol-saturated (EG) preparations of the Paleoproterozoic Francevillian Basin K-bentonites.

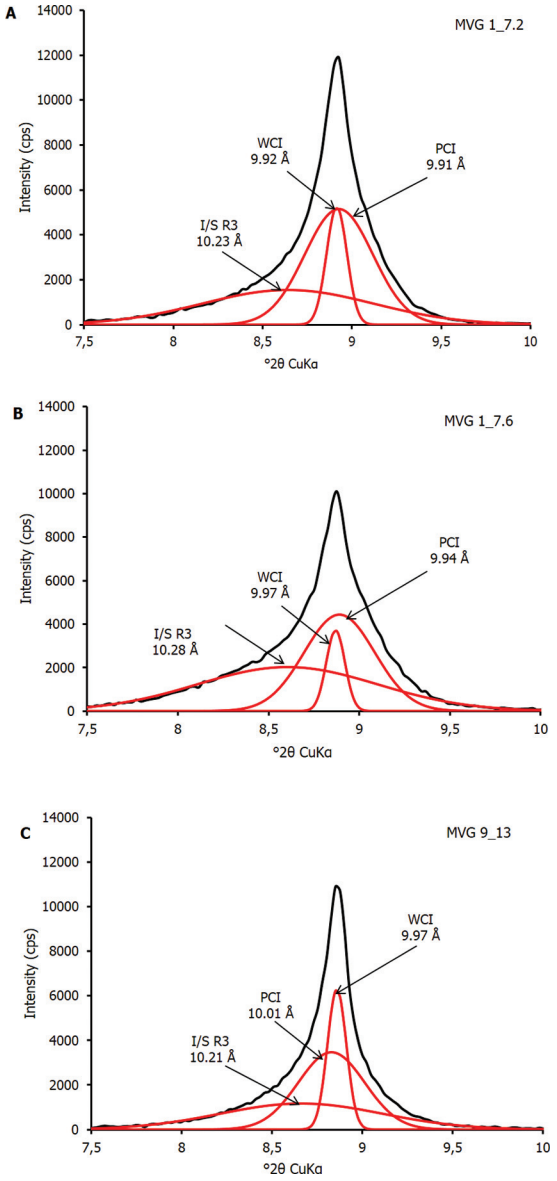

Fig. A-2. Decomposed 001 illite peaks of <2 μm clay fraction in ethylene-glycol (EG) preparations of the Paleoproterozoic Francevillian Basin K-bentonites: (A) MVG 1_7.2; (B) MVG 1_7.6; and (C) MVG 9_13. WCI peaks are narrow, while the PCI and I/S peaks are broad (WCI = well crystallized illite; PCI = poorly crystallized illite; I/S = illite-smectite mixed layer clay minerals).

REFERENCES

Bankole, O. M., El Albani, A., Meunier, A., and Gauthier-Lafaye, F., 2015, Textural and paleo-fluid flow control on diagenesis in the Paleoproterozoic Franceville Basin, South Eastern, Gabon: Precambrian Research, v. 268, p. 115–134, https://doi.org/10.1016/j.precamres.2015.07.008

Bankole, O. M., El Albani, A., Meunier, A., Rouxel, O. J., Gauthier-Lafaye F., and Bekker, A., 2016, Origin of red beds in the Paleoproterozoic Franceville Basin, Gabon, and implications for sandstone-hosted uranium mineralization: American Journal of Science, v. 316, n. 9, p. 839–872, https://doi.org/10.2475/09.2016.02

Batchelor, R. A., and Jeppsson, L., 1994, Late Llandovery bentonites from Gotland, Sweden, as chemostratigraphic markers: Journal of the Geological Society, London, v. 151, p. 741–746, https://doi.org/10.1144/gsjgs.151.5.0741

——— 1999, Wenlock metabentonites from Gotland, Sweden: Geochemistry, sources and potential as chemostratigraphic markers: Geological Magazine, v. 136, n. 6, p. 661–669, https://doi.org/10.1017/S001675689900285X

Bea, F., Montero, F., González-Lodeiro, F., and Talavera, C., 2007, Zircon inheritance reveals exceptionally fast crustal magma generation processes in Central Iberia during the Cambro-Ordovician: Journal of Petrology, v. 48, n. 12, p. 2327–2339, https://doi.org/10.1093/petrology/egm061

Bekker, A., Krapež, B., Müller, S., and Karhu, J. A., 2016, A short-term, post-Lomagundi positive C isotope excursion at *c.* ~2.03 Ga recorded by the Wooly Dolomite, Western Australia: Journal of the Geological Society, London, v. 173, n. 4, p. 689–700, https://doi.org/10.1144/jgs2015-152

Bonhomme, M. G., Gauthier-Lafaye, F., and Weber, F., 1982, An example of lower Proterozoic sediments: The Franceville in Gabon: Precambrian Research, v. 18, n. 1–2, p. 87–102, https://doi.org/10.1016/0301-9268(82)90038-9

Bouton, P., Thiéblemont, D., Gouin, J., Cocherie, A., Guerrot, C., Tegyey, M., Préat, A., Simo Ndounze, S., and Moussavou, M., 2009, Notice explicative de la carte géologique de la République du Gabon à 1/200 000, feuille Franceville-Boumango: Libreville, Edition DGMG-Ministère des Mines, du Pétrole, des Hydrocarbures, p. 1–79.

Brindley, G. W., and Brown, G., 1980, X-ray diffraction procedures for clay mineral identification, *in* Brindley, G. W., and Brown, G., editors, Crystal structures of clay minerals and their X-ray identification: Mineralogical Society, London, Monograph 5, p. 305–359.

Bros, R., Stille, P., Gauthier-Lafaye, F., Weber, F., and Clauer, N., 1992, Sm–Nd isotopic dating of Proterozoic clay material: An example from the Francevillian sedimentary series, Gabon: Earth and Planetary Science Letters, v. 113, n. 1–2, p. 207–218, https://doi.org/10.1016/0012-821X(92)90220-P

Brusewitz, A. M., 1988, Asymmetric zonation of a thick Ordovician K-bentonite bed at Kinnekulle, Sweden: Clays and Clay Minerals, v. 36, n. 4, p. 349–353, https://doi.org/10.1346/CCMN.1988.0360409

Caen-Vachette, M., Vialette, Y., Bassot, J. P., and Vidal, P., 1988, Apport de la geochronology isotopique à la connaissance de la géologie gabonaise: Chronique de la Recherche Minière, v. 491, p. 35–53.

Christidis, G. E., and Huff, W. D., 2009, Geological aspects and genesis of bentonites: Elements, v. 5, n. 2, p. 93–98, https://doi.org/10.2113/gselements.5.2.93

Clayton, T., Francis, J. E., Hillier, S. J., Hodson, F., Saunders, R. A., and Stone, J., 1996, The implications of reworking on the mineralogy and chemistry of Lower Carboniferous K-bentonites: Clay minerals, v. 31, p. 377–390, https://doi.org/10.1180/claymin.1996.031.3.08

D'Agrella-Filho, M. S., and Cordani, U. G., 2017, The paleomagnetic record of the São Francisco-Congo Craton, *in* Heilbron, M., Cordani U. G., and Alkmim F. F., editors, São Francisco Craton, Tectonic genealogy of a miniature continent, Eastern Brazil: Berlin, Springer International Publishing, Regional Geology Reviews, p. 305–320, https://doi.org/10.1007/978-3-319-01715-0_16

D'Agrella-Filho, M. S., Bispo-Santos, F., Trindade, R. I. F., and Antonio, P. Y. J., 2016, Paleomagnetism of the Amazonian Craton and its role in paleocontinents: Brazillian Journal of Geology, v. 46, n. 2, p. 275–299, https://doi.org/10.1590/2317-4889201620160055

Dai, S., Ward, C. R., Graham, I. T., French, D., Hower, J. C., Zhao, L., and Wang, X., 2017, Altered volcanic ashes in coal and coal-bearing sequences: A review of their nature and significance: Earth-Science Reviews, v. 175, p. 44–74, https://doi.org/10.1016/j.earscirev.2017.10.005

El Albani, A., Bengton, S., Canfield, D. E., Bekker, A., Miacchiarelli, R., Mazurier, A., Hammarlund, E. U., Boulvais, P., Dupuy, J. J., Fontaine, C., Fürsich, F. T., Gauther-Lafaye, F., Janvier, P., Javaux, E., Ossa-Ossa, F., Pierson-Wickmann, A. C., Riboulleau, A., Sardini, P., Vachard, D., Whitehouse, M., and Meunier, A., 2010, Large colonial organisms with coordinated growth in oxygenated environments 2.1 Gyr ago: Nature, v. 466, p. 100–104, https://doi.org/10.1038/nature09166

El Albani, A., Bengston, S., Canfield, D. E., Riboulleau, A., Bard, C. R., Macchiarelli, R., Pemba, L. N., Hammarlund, E., Meunier, A., Mouele, I. M., Benzerara, K., Bernard, S., Boulvais, P., Chaussidon, M., Cesari, C., Fontaine, C., Chi-Fru, E., Ruiz, J. M. G., Gauthier-Lafaye, F., Mazurier, A., Pierson-Wickmann, A. C., Rouxel, O., Trentesaux, A., Vecoli, M., Versteegh, G. J. M., White, L., Whitehouse, M., and Bekker, A, 2014, The 2.1 Ga Old Francevillian biota: Biogenicity, Taphonomy, and biodiversity: PLOS ONE, v. 9, n. 6, e99438, https://doi.org/10.1371/journal.pone.0099438

Fernandez-Alonso, M., Cutten, H., De Waele, B., Tacka, L., Tahon, A., Baudet, D., and Barritt, S. D., 2012, The Mesoproterozoic Karagwe-Ankole Belt (formerly the NE Kibara Belt): The result of prolonged extensional intracratonic basin development punctuated by two short-lived far-field compressional events: Precambrian Research, v. 216–219, p. 63–86, https://doi.org/10.1016/j.precamres.2012.06.007

Feybesse, J. L., Johan, V., Triboulet, C., Guerrot, C., Mayaga-Mikolo, F., Bouchot, V., and Eko N'dong, J., 1998, The West Central African Belt: A model of 2.5–2.0 Ga accretion and two-phase orogenic evolution: Precambrian Research, v. 87, n. 3–4, p. 161–216, https://doi.org/10.1016/S0301-9268(97)00053-3

Gauthier-Lafaye, F., 2006, Time constraint for the occurrence of uranium deposits and natural nuclear fission reactors in the Paleoproterozoic Franceville Basin (Gabon): Geological Society of America Memoir 198, p. 157–167, https://doi.org/10.1130/2006.1198(09)

Gauthier-Lafaye, F., and Weber, F., 1989, The Francevillian (Lower Proterozoic) Uranium ore deposits of Gabon: Economic Geology, v. 84, n. 8, p. 2267–2285, https://doi.org/10.2113/gsecongeo.84.8.2267

——— 2003, Natural nuclear fission reactors: Time constraints for occurrence, and their relation to uranium

and manganese deposits and to the evolution of the atmosphere: Precambrian Research, v. 120, n. 1–2, p. 81–100, https://doi.org/10.1016/S0301-9268(02)00163-8
Grathoff, G. H., and Moore, D. M., 1996, Illite polytype quantification using wildfire© calculated X-ray diffraction patterns: Clays and Clay Minerals, v. 44, n. 6, p. 835–842, https://doi.org/10.1346/CCMN.1996.0440615
Grim, R. E., and Güven, N., editors, 1978, Bentonites – Geology, Mineralogy, Properties, and Uses: New York, Elsevier, Developments in Sedimentology, v. 24, 256 p.
Guerra-Sommer, M., Cazzulo-Klepzig, M., Santos, J. O. S., Hartmann, L. A., and Ketzer, J. M., and Formoso, M. L. L., 2008, Radiometric age determination of tonsteins and stratigraphic constraints for the Lower Permian coal succession in southern Paraná Basin, Brazil: International Journal of Coal Geology, v. 74, n. 1, p. 13–27, https://doi.org/10.1016/j.coal.2007.09.005
Haubensack, C., ms, 1981, Environnement des grès protérozoıques et des indices uranifères du secteur Kiéné dans le bassin de Franceville (République Gabonaise): Aspects sédimentologiques et géochimiques: Strasbourg, France, Université de Strasbourg, Ph. D. thesis, 109 p.
Horie, K., Hidaka, H., and Gauthier-Lafaye, F., 2005, U-Pb Zircon geochronology of the Franceville series at Bidoudouma, Gabon: Goldschmidt Conference Abstract, Geochimica et Cosmochimica Acta, v. 69, A11.
Huff, W. D., 2008, Ordovician K-bentonites: Issues in interpreting and correlating ancient tephras: Quaternary International, v. 178, n. 1, p. 276–287, https://doi.org/10.1016/j.quaint.2007.04.007
——— 2016, K-bentonites: A review: American Mineralogist, v. 101, n. 1, p. 43–70, https://doi.org/10.2138/am-2016-5339
Huff, W. D., and Türkmenoglŭ, A. G., 1981, Chemical characteristics and origin of Ordovician K-bentonites along the Cincinnati Arch: Clays and Clay Minerals, v. 29, n. 2, p. 113–123, https://doi.org/10.1346/CCMN.1981.0290205
Huff, W. D., Morgan, D. J., and Rundle, C. C., 1996, Silurian K-bentonites of the Welsh Borderlands: Geochemistry, mineralogy and K-Ar ages of illitization: British Geological Survey, Report WG/96/045, 25 p., http://nora.nerc.ac.uk/id/eprint/7090
Huff, W. D., Bergstrom, S. M., Kolata, D. R., and Sun, H., 1998, The Lower Silurian Osmundsberg K-bentonite. Part II: Mineralogy, geochemistry, chemostratigraphy and tectonomagmatic significance: Geological Magazine, v. 135, n. 1, p. 15–26, https://doi.org/10.1017/S001675689700811X
Hurai, V., Paquette, J. L., Huraiova, M., and Konečný, P., 2010, U-Th-Pb geochronology of zircon and monazite from syenite and pincinite xenoliths in Pliocene alkali basalts of the intra-Carpathian back-arc basin: Journal of Volcanology and Geothermal Research, v. 198, n. 3–4, p. 275–287, https://doi.org/10.1016/j.jvolgeores.2010.09.012
Jackson, S. E., Pearson, N. J., Griffin, W. L., and Belousova, E.A., 2004, The application of laser ablation inductively coupled plasma-mass spectrometry to *in situ* U–Pb zircon geochronology: Chemical Geology, v. 211, n. 1–2, p. 47–69, https://doi.org/10.1016/j.chemgeo.2004.06.017
Karhu, J. A., and Holland, H. D., 1996, Carbon isotopes and the rise of atmospheric oxygen: Geology, v. 24, n. 10, p. 867–870, https://doi.org/10.1130/0091-7613(1996)024<0867:CIATRO>2.3.CO;2
Kiipli, T., Kallaste, T., and Nestor, V., 2010, Composition and correlation of volcanic ash beds of Silurian age from the eastern Baltic: Geological Magazine, v. 147, n. 6, p. 895–909, https://doi.org/10.1017/S0016756810000294
Kump, L. R., Junium, C., Arthur, M. A., Brasier, A., Fallick, A., Melezhik, V., Lepland, A., Črne, A.E., and Luo, G., 2011, Isotopic evidence for massive oxidation of organic matter following the Great Oxidation Event: Science, v. 334, n. 6063, p. 1694–1696, https://doi.org/10.1126/science.1213999
Leclerc, J., and Weber, F., 1980, Geology and genesis of the Moanda manganese deposits, Republic of Gabon, *in* Varentsov, I. M., and Grasselly, G., editors, Geology and Geochemistry of Manganese, Volume: Stuttgart, Germany, E. Schweizerbar'sche Verlagsbuchhandlung, p. 89–109.
Ludwig, K. R., 2001, User's manual for Isoplot/Ex Version 2.49, a geochronological toolkit for Microsoft Excel: Berkeley, California, Berkeley Geochronological Center, Special Publication 1a, 55 p.
Lustrino, M., and Wilson, M., 2007, The Circum-Mediterranean Anorogenic Cenozoic Igneous Province: Earth Science Reviews, v. 81, n. 1, p. 1–65, https://doi.org/10.1016/j.earscirev.2006.09.002
Martin, A. P., Condon, D. J., Prave, A. R., and Lepland, A., 2013, A review of temporal constraints for the Palaeoproterozoic large, positive carbonate carbon isotope excursion (the Lomagundi-Jatuli Event): Earth-Science Reviews, v. 127, p. 242–261, https://doi.org/10.1016/j.earscirev.2013.10.006
Martin, A. P., Prave, A. R., Condon, D. J., Lepland, A., Fallick, A. E., Romashkin, A. E., Medvedev, P. V., and Rychanchik, D. V., 2015, Multiple Palaeoproterozoic carbon burial episodes and excursions: Earth and Planetary Science Letters, v. 424, p. 226–236, https://doi.org/10.1016/j.epsl.2015.05.023
McDonough, W. F., and Sun, S. S., 1995, The composition of the Earth: Chemical Geology, v. 120, n. 3–4, p. 223–253, https://doi.org/10.1016/0009-2541(94)00140-4
McLennan, S. M., Hemming, S., McDaniel, D. K., and Hanson, G. N., 1993, Geochemical approaches to sedimentation, provenance, and tectonics, *in* Johnsson, M. J., and Basu, A., editors, Processes controlling the composition of clastic sediments: Geological Society of America Special Papers, v. 284, p. 21–40, https://doi.org/10.1130/SPE284-p21
Meunier, A., and Velde, B., 2004, Illite: Origins, Evolution and Metamorphism: Berlin, Springer-Verlag, 286 p., https://doi.org/10.1007/978-3-662-07850-1
Moe, J. A., Ryan, P. C., Elliott, W. C., and Reynolds, R. C., Jr., 1996, Petrology, chemistry, and clay mineralogy of a K-bentonite in the Proterozoic Belt Supergroup of western Montana: Journal of Sedimentary Research, v. 66, n. 1, p. 95–99, https://doi.org/10.1306/D42682C0-2B26-11D7-8648000102C1865D
Moore, D. M., and Reynolds, R. C., Jr., 1997, X-ray diffraction and the identification and analysis of clay minerals: Oxford, England, Oxford University Press, Second Edition, 378 p.
Moussavou, M., and Edou-Minko, A., 2006, Contribution à l'histoire thermo-tectonique précambrienne du

complexe annulaire de Ngoutou par la géochimie et la géochronologie U/Pb sur minéraux accessoires (Bassin Francevillien d'Okondja, Gabon): African Geoscience Review, v. 13, p. 53–61.

Ngombi-Pemba, L., El Albani, A., Meunier, A., Grauby, O., and Gauthier-Lafaye, F., 2014, From detrital heritage to diagenetic transformations: The message of clay minerals contained within shales of Paleoproterozoic Franceville Basin (Gabon): Precambrian Research, v. 255, p. 63–75, https://doi.org/10.1016/j.precamres.2014.09.016

Ossa Ossa, F. O., El Albani, A., Hofmann, A., Bekker, A., Gauthier-Lafaye, F., Pambo, F., Meunier, A., Fontaine, C., Boulvais, P., Pierson-Wickmann, A. C., Cavalazzi, B., and Macchiarelli, R., 2013, Exceptional preservation of expandable clay minerals in the *ca.* 2.1 Ga black shales of the Francevillian basin, Gabon and its implication for atmospheric oxygen accumulation: Chemical Geology, v. 362, p. 181–192, https://doi.org/10.1016/j.chemgeo.2013.08.011

Ovchinnikova, G. V., Kuznetsov, A. B., Melezhik, V. A., Gorokhov, I. M., Vasil'eva, I. M., and Gorokhovskii, B. M., 2007, Pb-Pb age of Jatulian carbonate rocks: The Tulomozero Formation of Southeast Karelia: Stratigraphy and Geological Correlation, v. 15, n. 4, p. 359–372, https://doi.org/10.1134/S0869593807040028

Paquette, J. L., and Mergoil-Daniel, J., 2009, Origin and U-Pb dating of zircon- bearing nepheline syenite xenoliths preserved in basaltic tephra (Massif Central, France): Contributions to Mineralogy and Petrology, v. 158, p. 245–262, https://doi.org/10.1007/s00410-009-0380-y

Paquette, J. L., Piro, J. L., Devidal, J. L., Bosse, V., Didier, A., Sannac, S., and Abdelnour, Y., 2014, Sensitivity enhancement in LA-ICP-MS by N_2 addition to carrier gas: Application to radiometric dating of U-Th-bearing minerals: Agilent ICP-MS Journal, v. 58, p. 4–5.

Pearce, J. A., Harris, N. B. W., and Tindle, A. G., 1984, Trace element discrimination diagrams for the tectonic interpretation of granitic rocks: Journal of Petrology, v. 25, n. 4, p. 956–983, https://doi.org/10.1093/petrology/25.4.956

Pickard, A. L., 2002, SHRIMP U-Pb zircon ages of tuffaceous mudrocks in the Brockman Iron Formation of the Hamersley Range, Western Australia: Australian Journal of Earth Sciences, v. 49, n. 3, p. 491–507, https://doi.org/10.1046/j.1440-0952.2002.00933.x

——— 2003, SHRIMP U-Pb zircon ages for the Palaeoproterozoic Kuruman Iron Formation, Northern Cape Province, South Africa: Evidence for simultaneous BIF deposition on Kaapvaal and Pilbara Cratons: Precambrian Research, v. 125, n. 3–4, p. 275–315, https://doi.org/10.1016/S0301-9268(03)00113-X

Préat, A., Bouton, P., Thiéblemont, D., Prian, J. P., Ndounze, S. S., and Delpomdor, F., 2011, Paleoproterozoic high $\delta^{13}C$ dolomites from the Lastoursville and Franceville basins (SE Gabon): Stratigraphic and syn-sedimentary subsidence implications: Precambrian Research, v. 189, n. 1–2, p. 212–228, https://doi.org/10.1016/j.precamres.2011.05.013

Sawaki, Y., Moussavou, M., Sato, T., Suzuki, K., Ligna, C., Asanuma, H., Sakata, S., Obayashi, H., Hirata, T., and Edou-Minko, A., 2017, Chronological constraints on the Paleoproterozoic Francevillian Group in Gabon: Geoscience Frontiers, v. 8, n. 2, p. 397–407, https://doi.org/10.1016/j.gsf.2016.10.001

Saylor, B. Z., Poling, J. M., and Huff, W. D., 2005, Stratigraphic and chemical correlation of volcanic ash beds in the terminal Proterozoic Nama Group, Namibia: Geological Magazine, v. 142, n. 5, p. 519–538, https://doi.org/10.1017/S0016756805000932

Sinclair, H. D., and Naylor, M., 2012, Foreland basin subsidence driven by topographic growth versus plate subduction: Geological Society of America Bulletin, v. 124, n. 3–4, p. 368–379, https://doi.org/10.1130/B30383.1

Spears, D. A., 2012, The origin of tonsteins, an overview, and links with seatearths, fireclays and fragmental clay rocks: International Journal of Coal Geology, v. 94, p. 22–31, https://doi.org/10.1016/j.coal.2011.09.008

Stille, P., Gauthier-Lafaye, F., and Bros, R., 1993, The neodynium isotope system as a tool for petroleum exploration: Geochimica et Cosmochimica Acta, v. 57, n. 18, p. 4521–4525, https://doi.org/10.1016/0016-7037(93)90502-N

Su, W., Zhang, S., Huff, W. D., Li, H., Ettenshon, F. R., Chen, X., Yang, H., Han, Y., Song, B., and Santosh, M., 2008, SHRIMP U–Pb ages of K-bentonite beds in the Xiamaling Formation: Implications for revised subdivision of the Meso- to Neoproterozoic history of the North China Craton: Gondwana Research, v. 14, n. 3, p. 543–553, https://doi.org/10.1016/j.gr.2008.04.007

Suganuma, Y., Okada, M., Horie, K., Kaiden, H., Takehara, M., Senda, R., Kimura, J., Kawamura, K., Haneda, Y., Kazaoka, O., and Head, M. J., 2015, Age of Matuyama-Brunhes boundary constrained by U-Pb zircon dating of a widespread tephra: Geology, v. 43, n. 6, p. 491–494, https://doi.org/10.1130/G36625.1

Taylor, S. R., and McLennan, S. M., 1985, The Continental Crust: Its Composition and Evolution: Oxford, England, Blackwell Scientific Publications, 312 p.

Thiéblemont, P., Castaing, C., Billa, M., Bouton, P., and Préat, A., 2009, Notice explicative de la carte géologique et des ressources minerales de la Republique Gabonaise: BRGM-Ministere des Mines, des Hydrocarbures, Libreville, scale 1:1000000, 1 sheet.

Thiéblemont, D., Boulton, P., Préat, A., Goujou, J. C., Tegyey, M., Weber, F., Ebang Obiang, E., Joron, J. L., and Treuil, M., 2014, Transition from alkaline to calc-alkaline volcanism during evolution of the Paleoproterozoic Franceville Basin of eastern Gabon (Western Central Africa): Journal of African Earth Sciences, v. 99, Part 2, p. 215–227, https://doi.org/10.1016/j.jafrearsci.2013.12.007

Van Achterbergh, E., Ryan, C. G., Jackson, S. E., and Griffin, W. L., 2001, Data reduction software for LA-ICP-MS, *in* Sylvester, P., editor, Laser ablation-ICPMS in the earth sciences: Ottawa, Ontario, Canadian Mineralogical Association of Canada Short Course Series29, p. 239–243.

Velde, B., and Vasseur, G., 1992, Estimation of the diagenetic smectite to illite transformation in time-temperature space: American Mineralogist, v. 77, n. 9–10, p. 967–976.

Weber, F., ms, 1968, Une série précambrienne du Gabon: le Francevillien, sédimentologie, géochimie, relations avec les gites minéraux: Strasbourg, France, Université de Strasbourg, Ph. D. thesis, 372 p.

Weber, F., Gauthier-Lafaye, F., Whitechurch, H., Ulrich, M., and El Albani, A., 2016, The 2-Ga Eburnean Orogeny in Gabon and the opening of the Francevillian intracratonic basins: A review: Comptes Rendus Geoscience, v. 348, n. 8, p. 572–586, https://doi.org/10.1016/j.crte.2016.07.003

Wiedenbeck, M., Allé, P., Corfu, F., Griffin, W. L., Meier, M., Oberli, F., von Quadt, A., Roddick, J. C., and Spiegel, W., 1995, Three natural zircon standards for U-Th-Pb, Lu-Hf, trace element and REE analyses: Geostandards Newsletter, v. 19, n. 1, p. 1–23, https://doi.org/10.1111/j.1751-908X.1995.tb00147.x

Winchester, J. A., and Floyd, P. A., 1977, Geochemical discrimination of different series and their differentiation products using immobile elements: Chemical Geology, v. 20, p. 325–343, https://doi.org/10.1016/0009-2541(77)90057-2